View metadata, citation and similar papers at core.ac.uk
brought to you by CORE
provided by NASA Technical Reports Server

research report

RECEIVED
APR 1969
NASA STI FACILITY
INPUT BRANCH

**WYLE LABORATORIES**
TESTING DIVISION, HUNTSVILLE FACILITY

FACILITY FORM 602

N69-25247
(ACCESSION NUMBER)
54
(PAGES)
CR-98418
(NASA CR OR TMX OR AD NUMBER)
(THRU)
1
(CODE)
23
(CATEGORY)

Reproduced by the
CLEARINGHOUSE
for Federal Scientific & Technical
Information Springfield Va. 22151

507 57018

WYLE LABORATORIES - RESEARCH STAFF

REPORT WR 68-12

# FORCES ACTING ON STATIONARY AND MOVING SOLID OBSTACLES IN PLANE WAVE SOUND FIELDS

By

L. C. Sutherland

Work Performed Under Contract NAS8-21260

October 1968

WYLE LABORATORIES

RESEARCH DIVISION, HUNTSVILLE FACILITY

COPY NO. 48

# ABSTRACT

The acoustic loads on unbaffled obstacles can be represented, to a first approximation, by the acoustic force acting on solid cylinders and spheres in plane wave sound fields. The well known theory for these cases is reviewed in a consistent manner to clarify physical interpretation and correct minor discrepancies in the literature. Limited experimental data, available from the literature, is used to illustrate the validity of the theory.

Motion of a solid obstacle in a sound field is shown to be dependent on the force acting on the obstacle when it is fixed. Finally, the theory for acoustic radiation reaction forces and viscous or aerodynamic forces acting on oscillating bodies is briefly reviewed along with some published experimental data for the viscous or aerodynamic forces acting on oscillating spheres, cylinders, and thin plates.

TABLE OF CONTENTS

## LIST OF FIGURES

## LIST OF SYMBOLS

| | |
|---|---|
| $A$ | Acceleration in g's |
| $A_n$ | Area normal to incident ray |
| $C_m(ka)$ | Modulus of mth order complex function of ka in expression for cylindrical pressure field |
| $D_m(ka)$ | Modulus of mth order complex function of ka in expression for spherical pressure field |
| $F$ | Force |
| $H'_m(z)$ | Bessel Function of third kind, mth order and argument (z) |
| $J_n(z)$ | Bessel Function of first kind, nth order and argument (z) |
| $K$ | Constant |
| $L_i$ | Acoustic force coupling factor for incident pressure field only |
| $L_t$ | Acoustic force coupling factor for total pressure on obstacle |
| $M$ | Mass of air in volume equal to obstacle volume |
| $P$ | Pressure amplitude |
| $P_m(\cos \phi)$ | Legendre Function of order m |
| $R$ | Mechanical resistance |
| $S$ | Total surface area |
| $V$ | Velocity amplitude |
| $X$ | Mechanical reactance |
| $Y_n(z)$ | Bessel Function of second kind, nth order and argument (z) |
| $Z$ | Mechanical impedance |

LIST OF SYMBOLS (Continued)

| | |
|---|---|
| $a$ | Radius of cylinder or sphere |
| $a_m$ | mth order constant |
| $c$ | Speed of sound |
| $c$ | Damping constant |
| $e$ | Napierian log base |
| $f$ | Frequency, Hz |
| $g$ | Acceleration of gravity |
| $h'_m(z)$ | Spherical Bessel Function of third kind, order m, and equal to $j_m(z) + i\ y_m(z)$ |
| $i$ | $= \sqrt{-1}$ |
| $j_m(z)$ | Spherical Bessel Function of first kind, order m, and argument (z) |
| $k$ | Wave number $\doteq 2\pi f/c$ |
| $\ell$ | Length of cylinder |
| $m$ | Mass |
| $m$ | Integer |
| $n$ | Integer |
| $p$ | Instantaneous acoustic pressure |
| $r$ | Radius from center of obstacle |
| $t$ | Time |
| $x$ | Rectangular coordinate, direction of plane wave |
| $y_m(z)$ | Spherical Bessel Function of second kind, order m, and argument (z) |
| $z$ | Dummy variable, usually used in place of ka |
| $z$ | Axial coordinate in cylindrical coordinate system |

## LIST OF SYMBOLS (Continued)

Subscripts

| | |
|---|---|
| a | Acoustical |
| d | Aerodynamic resistance |
| i | Incident |
| m | Mechanical |
| o | Amplitude |
| r | Radiation |
| s | Scattered |
| t | Total (incident plus scattered) |
| v | Viscous resistance |

Greek Symbols

| | |
|---|---|
| $\alpha$ | Angular function of ka in expression for acoustic force on sphere |
| $\beta$ | Angle of incidence in XZ (vertical) plane for oblique plane wave inc on cylinder |
| $\gamma_m(ka)$ | mth order phase term in expression for cylindrical pressure field |
| $\delta_m(ka)$ | mth order phase term in expression for spherical pressure field |
| $\theta$ | Angle in cylindrical coordinates in plane normal to cylinder axis |
| $\lambda$ | Wavelength = c/f |
| $\nu$ | Kinematic viscosity |
| $\rho$ | Mass density of medium |
| $\phi$ | Polar angle relative to the direction of an incident wave on a sphere |
| $\omega$ | Frequency, radians/sec |

# 1.0 INTRODUCTION

Obstacles placed in a sound field are acted on by oscillating forces due to an unbalanced distribution of the incident and scattered sound pressures on the surface of the obstacles. Most of the current theoretical studies on response of structure to acoustic noise are concerned with acoustic loads on only one side of a structural surface. This is realistic when one side of a structure is isolated from significant excitation. However, tall buildings, tank structures, ground equipment racks, etc., are examples of unbaffled obstacles for which the net acoustical load depends on the pressure distribution on all sides of the structure. For example, acoustic excitation of the fundamental bending mode of a nine-story building has been observed due to acoustic excitation during static firing of large rocket engines. It is the purpose of this brief study to consider acoustic forces and resulting motion of infinite circular cylinders and rigid spheres. These two cases can be considered as first approximations for defining acoustic loads on three-dimensional objects.

The scattering theory employed in this study has been well developed by Morse (Reference 1), Lindsay (Reference 3), and Rschevkin (Reference 5) and is not repeated in detail here. Rather, the objective has been to define the essential features of the results in a consistent manner and, in some cases, extend the results beyond those found in these references, stressing their physical interpretation. Some minor inconsistencies relative to this report in References 1 and 5 are also clarified and corrected.

In Sections 2 and 3, methods for approximating the exact solution for the net acoustic force on cylinders and spheres are also covered since these can often be used to advantage under certain conditions. In one approximation, it is shown that when scattering is neglected, the acoustic force on the cylinder and sphere, at wavelengths large relative to the obstacle circumference, are 1/2 and 2/3, respectively, of the true value. For this reason, it is suggested that a numerical integration of only incident pressures on an irregular shape body could be used to estimate the net acoustic force within an accuracy of ± 17 percent (± 1.4 dB) for a solid obstacle whose circumference is less than the incident wavelength.

In Section 4, translational motion of a sphere in an acoustic field is considered. It is shown that the motion of the sphere can be accurately determined by defining the net acoustic force on the obstacle when it is rigid. This concept is a general one applicable for defining the motion of any obstacle in an acoustic field. In Section 5, available experimental data on the motion of unbaffled obstacles in a sound field are compared with the theoretical results and reasonable agreement between theory and experiment is demonstrated. Finally, in Section 6, the additional effect of viscous drag forces on the translational motion of spheres ... is briefly reviewed and a comparison of theory with published e... ustrated. It is shown that the theory accurately predicts a drag ... treated as a linear viscous damping force for small amplitude...

Two appendices are included. Appendix A covers some of the derivatives omitted from the text. Appendix B summarizes the radiation impedance expressions, and their high and low frequency asymptotes for oscillating and pulsating spheres and cylinders.

## 2.0 ACOUSTIC FORCE ON A RIGID INFINITE CYLINDER IN A PLANE WAVE SOUND FIELD

### 2.1 Net Force on Cylinder Without Considering Scattering

Consider a plane acoustic wave of angular frequency $\omega$ and wave number $k = \omega/c$ traveling to the right and incident upon an infinite circular cylinder of radius a whose axis is at right angles to the incident sound direction. As indicated in the following sketch, the incident pressure, $p_i$ at a point a, $\theta$ on the surface of the cylinder at an angle $\theta$ from the incident ray direction can be expressed in the complex form (Reference 1)*

$$p_i = P_0 \; e^{-i(\omega t - ka \cos \theta)} \tag{1}$$

where ka is the dimensionless frequency $\omega a/c$.

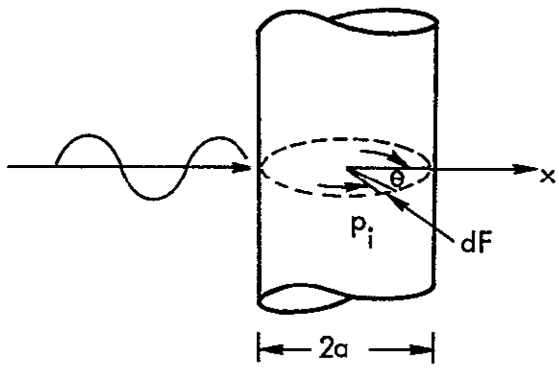


For a first approximation, the net force on the cylinder is defined by neglecting the scattered pressure at the cylinder surface. If a positive pressure on the cylinder implies a radial force directed inward, the instantaneous radial force, due to the incident pressure only, on a surface element of unit axial length and length $a\,d\theta$ around the circumference is given by

$$dF_i = P_0 \; e^{-i(\omega t - ka \cos \theta)} \; a \, d\theta \tag{2}$$

---

* The convention of using $e^{-i\omega t}$ instead of $e^{j\omega t}$ is adopted from Morse. Rschevkin employs the latter convention and his results are equivalent to Morse's when j, the positive root of $\sqrt{-1}$, is replaced by $-i$, the negative root of $\sqrt{-1}$.

If force is positive in the direction of travel of the incident wave, the instantaneous value of the net horizontal force is

$$F_i = -2a\,P_0 \left[\int_0^{\pi} e^{i\,ka\cos\theta}\cos\theta\,d\theta\right] e^{-i\omega t} \tag{3}$$

The integral has a known solution in the form (Reference 2)

$$\frac{i^{-n}}{\pi}\int_0^{\pi} e^{i\,z\cos\theta}\cos(n\theta)\,d\theta = J_n(z) \tag{4}$$

where $J_n(z)$ is the nth Bessel Function of the first kind and argument z

Thus, utilizing Equation 4 in Equation 3, the expression for the complex value of the net force is:

$$F_i = -\,i\,2\pi\,a\,P_0\,J_1\,(ka)\,e^{-i\omega t} \tag{5}$$

Using the relationship $-\,i = e^{-i\,\pi/2}$, the real part of the instantaneous force can be expressed as:

$$F_i = 2a\,P_0\,[\pi\,J_1(ka)]\,\cos(\omega t + \pi/2) \tag{6}$$

At the plane passing through the axis of the cylinder for $\theta = \pi/2$, the real value of the instantaneous incident pressure, from Equation 1, is

$$p_i = P_0\,\cos\omega t$$

Comparing this with Equation 6, it is clear that the net acoustic force, based on the incident pressure only, <u>leads</u> the incident pressure at the center of the cylinder by $\pi/2$ radians or 1/4 of the period. This is illustrated graphically in Figure 1 which shows the pressure distribution and net force on the cylinder at different times. This same leading phase will still hold when the scattered wave is included in the analysis and $ka << 1$. Some inconsistency on this point appears on page 353 of Reference 1 and is repeated in Reference 5 in the derivation of the net force on a cylinder. The source of the inconsistency appears to be the omission in each of these references of a minus sign in the basic equation for the net force. This minus sign is required if the net force is considered positive in the direction of travel of the incident wave; $\theta = 0$.

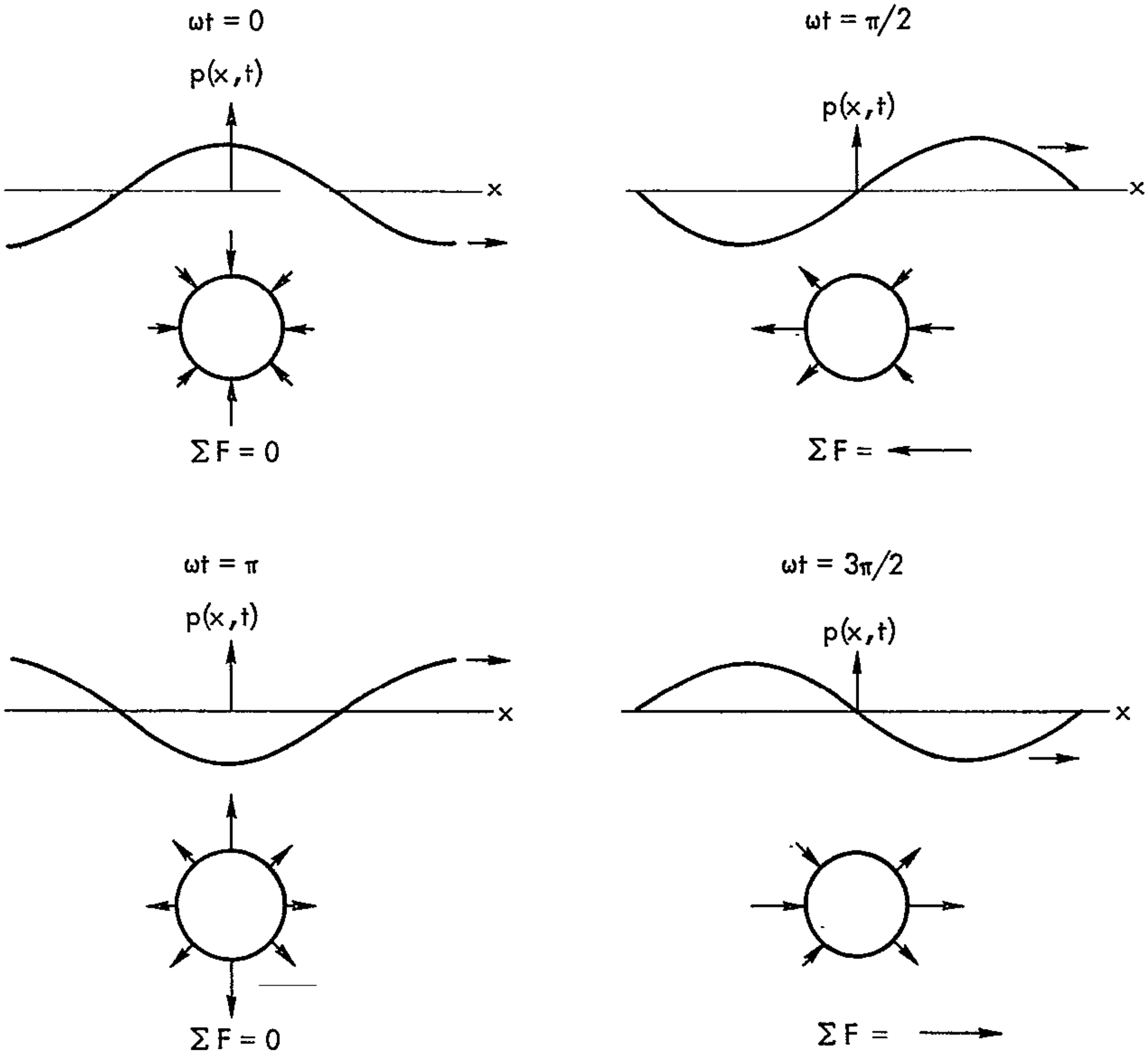


a. Spatial Distribution and Net Summation of Incident Pressure

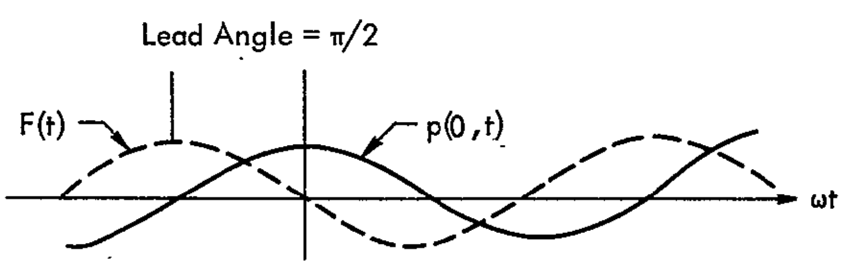


b. Time Variation of Incident Pressure and Net Acoustic Force

Figure 1. Space and Time Variation of Incident Pressure at Center of Cylinder

If the net force is normalized by the product of the reference incident pressure, $p_i$, and the area normal to the plane wave (2a per unit length), then an acoustic force coupling factor can be expressed as the complex ratio

$$L_i = \frac{\text{Net Force}}{\text{Normal Area x Incident Pressure}} = \pi J_1(ka)\, e^{-i\pi/2} \tag{7}$$

Due to the omission of the scattered sound pressure at the surface of the cylinder, this expression is not exact. We would expect, however, that it would be a reasonable first approximation at frequencies for which the wavelength is much greater than the cylinder circumference ($ka << 1$). In this case, the Bessel Function may be approximated by its first series term so that the magnitude of $L_i$ is approximately

$$L_i \cong \pi \frac{ka}{2}\, e^{-i\pi/2}, \qquad ka << 1 \tag{8}$$

The following section will show that in the low frequency range, the effect of scattering increases the net acoustic force by a factor of 2 over that computed above on the basis of the incident pressure only.

## 2.2 Net Force on Cylinder Including Effect of Scattering

The total pressure, $p_t$, at any point on the surface of the cylinder will be the sum of the incident plus scattered or reflected pressure, $p_s$

$$p_t = P_0\, e^{-i(\omega t - ka\cos\theta)} + p_s \tag{9}$$

The scattered pressure is determined by satisfying the boundary condition at the surface of the rigid cylinder that the particle velocity normal to the surface must be zero. A formal solution for this problem has been presented by Morse (Reference 1), Lindsay (Reference 3), and Rschevkin (Reference 5)

The solution involves first defining the incident plane wave in cylindrical coordinates Then, assuming a general solution in cylindrical coordinates for the scattered sound field, the coefficients of this solution are defined so that the radial velocity component of the scattered field on the surface of the cylinder just cancels the radial velocity component of the incident wave to satisfy the boundary condition of zero velocity at the surface of the cylinder

Based on this method, the sum of the incident plus scattered pressure on the cylinder surface at an angle θ relative to the propagation direction of the incident plane wave is given by (References 1 and 3)

$$p_t = p_i + p_s = \frac{4P_0}{\pi ka} e^{-i\omega t} \sum_{m=0}^{\infty} \frac{\cos m\theta \, e^{i m \pi/2}}{C_m \, e^{i\gamma_m}} \tag{10}$$

where the function $C_m e^{i\gamma_m}$ is equal to

$$C_m e^{i\gamma_m} = \begin{cases} -2\left[Y_1(ka) - i\,J_1(ka)\right] & m = 0 \\ \frac{1}{2}\left[Y_{m-1}(ka) - Y_{m+1}(ka) + i\,J_{m+1}(ka) - i\,J_{m-1}(ka)\right] & m > 0 \end{cases} \tag{11}$$

and

$J_m(ka)$ = Bessel Function of the first kind

$Y_m(ka)$ = Bessel Function of the second kind (also called Neumann or Weber Function)

It should be noted that in Equation 11, $C_m$ is the real modulus of the complex quantity on the right side and $e^{i\gamma_m}$ is the unit complex vector representing its phase angle. Morse has tabulated values of $C_m$ and $\gamma_m$ for a range of the argument ka from 0 to 5 and for m = 0 to 9 (Reference 1).

Weiner (Reference 4) has calculated, and confirmed by measurement, the ratio of total to incident pressure for a cylinder. His theoretical results are shown in Figure 2. Limiting values of $C_m$ and $\gamma_m$ for very small or very large values of ka are given by Morse in the following form

For $ka << m + 1/2$,

$$\begin{aligned} m = 0, \quad & C_0 \simeq 4/\pi ka, & \gamma_0 \simeq \pi (ka/2)^2 \\ m > 0, \quad & C_m \simeq \frac{m!}{2\pi} (2/ka)^{m+1} & \gamma_m \simeq -\frac{\pi m}{(m!)^2} (ka/2)^{2m} \end{aligned} \tag{11a}$$

For $ka >> m + 1/2$,

$$\begin{aligned} m = 0, \quad & C_0 \simeq \sqrt{8/\pi ka}, & \gamma_0 \simeq ka - \pi/4 \\ m > 0, \quad & C_m \simeq \sqrt{2/\pi ka}, & \gamma_m \simeq ka - \frac{\pi}{2}(m + 1/2) \end{aligned} \tag{11b}$$

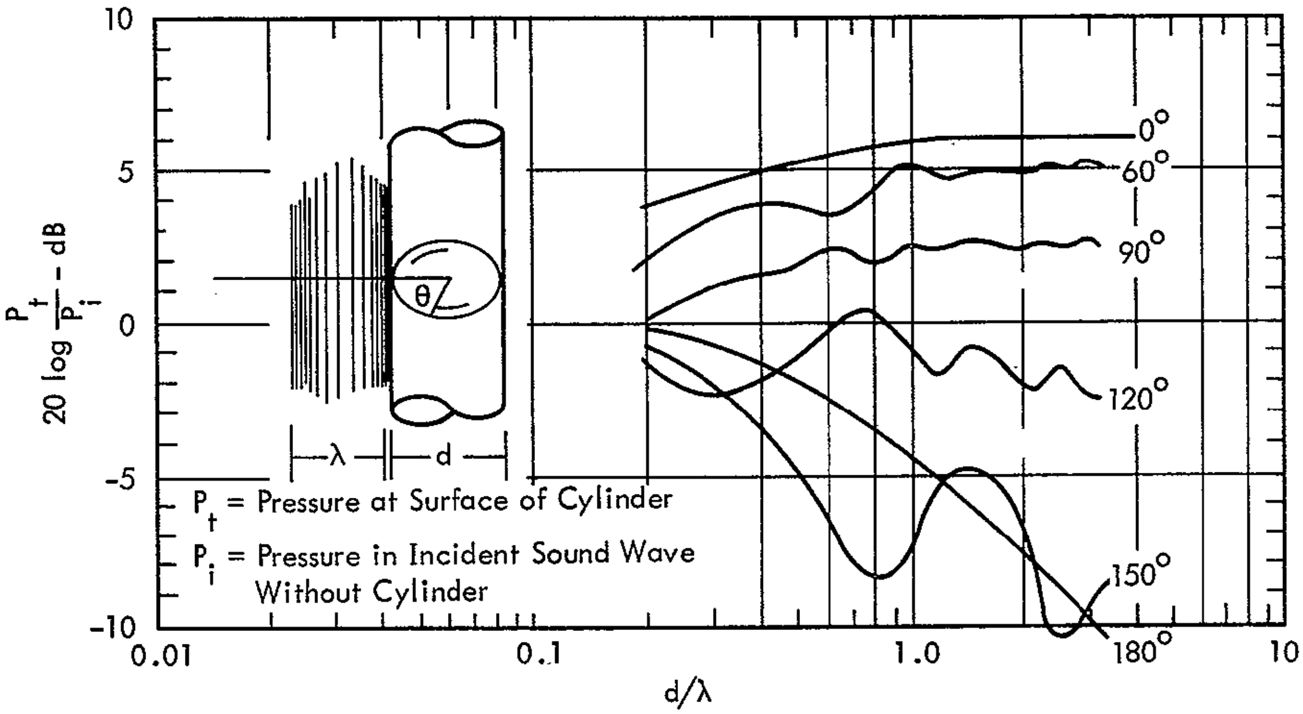


Figure 2. Pressure Distribution Around Cylinder for Normally Incident Plane Wave (From Weiner, Reference 4)

The approximation for large ka is difficult to employ for estimating the trend in $p_t$ at high frequencies since it becomes less accurate as more terms are required in the summation in Equation 10. A plot of the amplitude each of the first 5 terms of the series in Equation 10 which defines the total pressure around the cylinder is given in Figure 3. Each term has an amplitude equal to $4/\pi$ ka $C_m$. It is clear that for small values of the dimensionless frequency parameter ka, just the first two terms will provide a reasonable approximation of the total pressure. Using these first two terms, when ka << 1,

$$p_t \simeq P_0 \ (1 + i\, 2\, ka \cos\theta)\, e^{-i\omega t} \qquad ka << 1 \tag{12}$$

One can also write the incidence wave pressure from Equation 1 in the approximate form for ka << 1, as

$$p_i \simeq P_0 \ (1 + i\, ka \cos\theta)\, e^{-i\omega t} \qquad ka << 1 \tag{13}$$

Thus, as pointed out by Morse (Reference 1), the scattered sound pressure at long wavelengths, adds a component to the incident pressure which is just equal to the complex or quadrature component of the incident pressure around the cylinder surface.

For high frequencies, where ka >> 1, Figure 3 clearly shows the increasing significance of higher order terms in the series expression of Equation 10.

To define the net force on the cylinder, it is necessary, as before, to integrate the instantaneous resultant force due to the incident plus scattered pressure over a unit length of the cylinder. This is given by

$$F_t = -2\, a \int_0^{\pi} p_t \cos\theta \, d\theta$$

Substituting in Equation 10, the result is an exact expression for the net force given by

$$F_t = 2\, a\, P_0 \left[ \frac{2}{ka\, C_1}\, e^{-i(\gamma_1 + \pi/2)} \right] e^{-i\omega t} \tag{14}$$

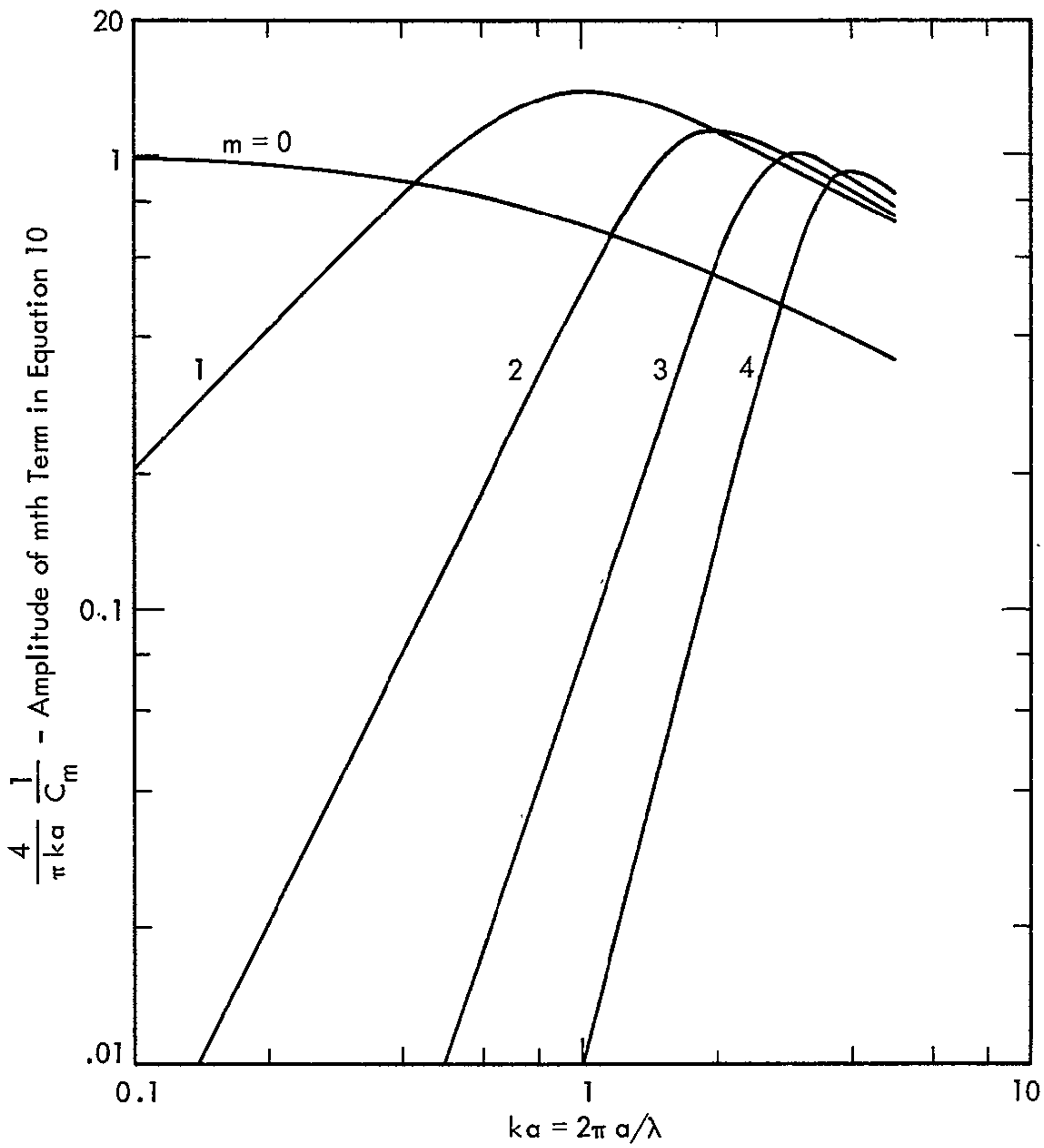


Figure 3. Amplitude of First Five Terms in Infinite Series Defining Incident Plus Scattered Pressure on Cylinder in Plane Wave Sound Field

where

$$C_1 = \frac{1}{2}\left\{\left[Y_0(ka) - Y_2(ka)\right]^2 + \left[J_2(ka) - J_0(ka)\right]^2\right\}^{\frac{1}{2}}$$

and

$$\gamma_1 = \tan^{-1}\left[\frac{J_2(ka) - J_0(ka)}{Y_0(ka) - Y_2(ka)}\right] \qquad (15)$$

Note that while an infinite series is required to define the total pressure on the cylinder, upon integration over the surface, all terms but the first order ($m = 1$) term drop out. This is expected since for the zero order term, there is no angular dependency of the total pressure, and hence no net unbalanced force. For higher order terms, the integral of $\cos m\theta \cos \theta$ over the limits of 0 to $\pi$ is zero for $m \neq 1$, so that these terms drop out.

Again, the net force can be normalized by the product of the incident pressure and the normal area to give an acoustic force coupling factor,

$$L_t = \frac{2}{ka\, C_1}\, e^{-i(\pi/2 + \gamma_1)} \qquad (16)$$

The amplitude and phase of the coupling factors defined by Equation 16 (with diffraction) and Equation 7 (without diffraction) are plotted in Figures 4 and 5, respectively.

As shown in Figure 4, the maximum value of the acoustic force coupling factor is 2.15 and it occurs at a value of $ka = 1$. This corresponds to a half wavelength equal to one half the circumference of the cylinder. Thus, as one might estimate, intuitively, the maximum force on the cylinder is approximately equal to two times the incident "force" (incident pressure times normal area) at the wavelength for which the incident pressures on the front and back of the cylinder are just 180 degrees out of phase. The net front-to-back pressure differential would then be twice the incident pressure. It will be shown in the next section that this qualitative concept of the net force on the cylinder can be used as a basis for a good approximation of the net force at all wavelengths greater than the circumference of the cylinder.

For very small and very large values of ka, utilizing Equation 11a and 11b, the coupling factor is approximately equal to

$$L_t \simeq \begin{cases} \pi\, ka\, e^{-i\pi/2} & ka \ll 1 \\ \sqrt{2\pi/ka}\, e^{-i(ka - \pi/4)}, & ka \gg 1 \end{cases} \qquad (17)$$

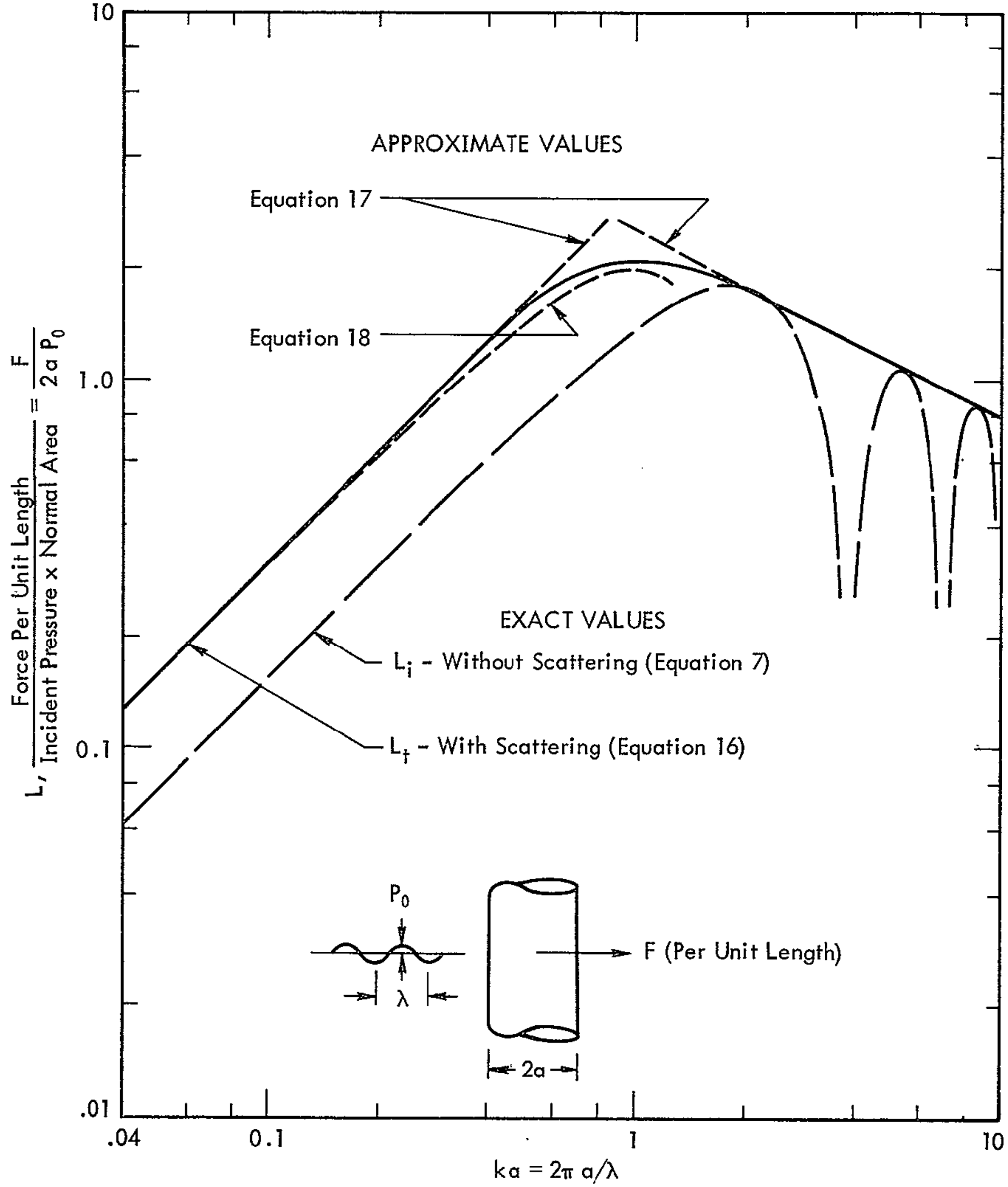


Figure 4. Acoustic Force Coupling Factor for Rigid Circular Cylinder in Plane Wave at Normal Incidence

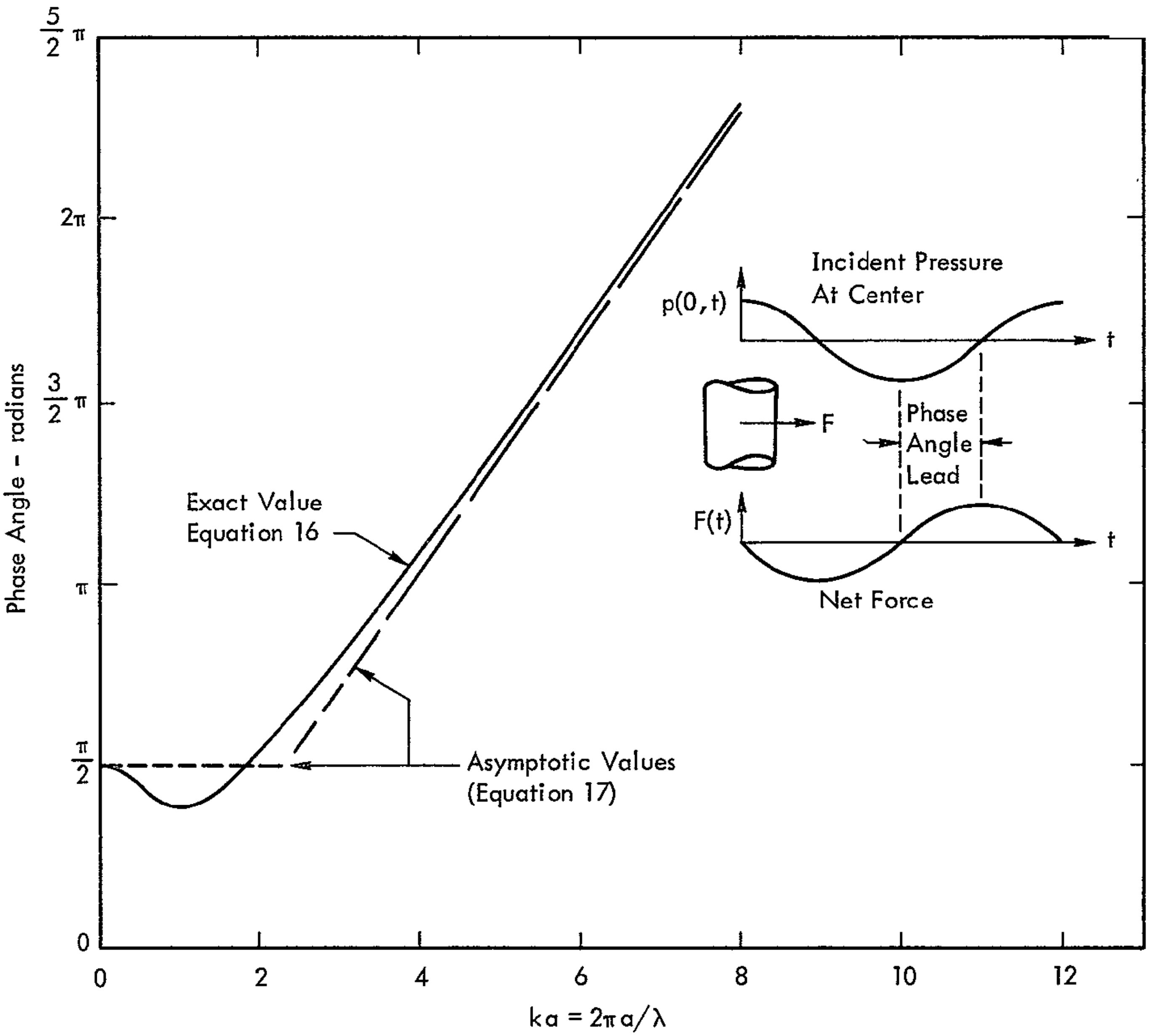


Figure 5. Phase Angle Between Acoustic Force on Cylinder and Normally Incident Plane Wave Referred to Center of Sphere

Comparing the asymptotic value above for small ka with that shown in Equation 8 where scattering was neglected, we see that the latter estimate is just 1/2 of the true value for ka << 1. This is clearly shown in Figure 4. It is also important to note that the upper envelope of the coupling factor, for large ka, computed without accounting for scattering, is essentially the same as the true value. This is a significant result which shows that, at high frequencies, the scattered pressure field on an obstacle has a net force of zero and the upper bound for the force is defined by the incident field only.

## 2.3 Approximate Method for Estimating Force on Cylinder

An approximate method is considered for estimating the force on the cylinder for ka << 1. A similar approach may be feasible for other obstacles.

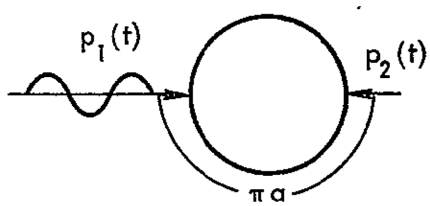


$$p_2(t) = p_1\left(t - \frac{\pi a}{c}\right)$$

Assume that the net force is the difference between the pressure at the point of incidence on the cylinder and the diametrically opposite point times the normal area (2a per unit length) of the cylinder. Furthermore, as shown in the sketch, assume that the phase difference between these two points is due to the circumferential path length $\pi a$ from front to back of the cylinder. If the axis of the cylinder is the center of the coordinate system, then the approximate net force over a unit length in the direction of the incident wave is:

$$F_t \simeq 2a\,[p_1(t) - p_2(t)] = 2a\,P_0\,[\cos(\omega t + ka) - \cos(\omega t + ka - \pi\,ka)]$$

which reduces to

$$F_t \simeq 2a\,P_0\left[2\sin\frac{(\pi\,ka)}{2}\right]\cos\left(\omega t + ka - \frac{\pi}{2}\,ka + \frac{\pi}{2}\right) \tag{18}$$

Thus, the acoustic coupling factor is

$$L_t \simeq \frac{F_t}{2a\,p_i} \simeq 2\sin\frac{\pi\,ka}{2}\,e^{-i[\pi/2 - ka(\pi/2 - 1)]} \qquad ka << 1 \tag{19}$$

For small values of ka, this becomes

$$L_t \simeq \pi\,ka\,e^{-i\pi/2} \tag{20}$$

which is the same as the low frequency approximation for the exact solution with diffraction (Equation 17). The approximation given by Equation 19 is also shown in Figure 4

## 2.4 Net Force on Cylinder for an Oblique Incident Wave

The discussion up till now has covered only the case for an incident wave traveling at right angles to the axis of the cylinder. It is also desirable to consider the case of an oblique wave incident on the cylinder. This case is illustrated in the following sketch.

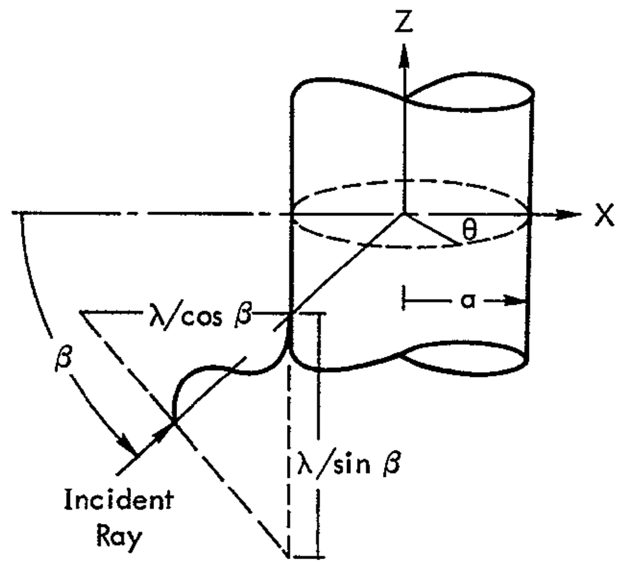


If an incident ray in the XZ plane intersects the cylinder axis (Z axis) at an angle $\beta$ to the normal (X axis) to the cylinder axis, the incident pressure can be defined by

$$p_i = P_0 \, e^{-i(\omega t - kx\cos\beta - kz\sin\beta)} \qquad (21)$$

At any circumferential point $(a, \theta)$ on the surface of the cylinder at a longitudinal station z, the incident pressure on the cylinder is given by

$$p_i(a,\theta,z) = \left[P_0 \, e^{-i(\omega t - ka\cos\beta\cos\theta)}\right] e^{ikz\sin\beta} \qquad (22)$$

Thus, the incident pressure on any circumferential ring for an oblique wave is given by the expression for the pressure of a normally incident wave (Equation 1) with k replaced by $k\cos\beta$, multiplied by the quantity $e^{ikz\sin\beta}$. Note that replacing k by $k\cos\beta$ is equivalent to saying that the effective wavelength in the direction normal to the cylinder is $\lambda/\cos\beta$ as shown in the above sketch. Similarly, $\lambda/\sin\beta$ is the effective or trace wavelength along the cylinder axis so that the additional term $e^{ikz\sin\beta}$ simply defines the additional phase shift of the incident pressure in the axial direction.

Wenzel has shown that the same result is obtained for the scattered pressure field for an oblique wave (Reference 7). Thus, the incident plus scattered pressure on the surface of a cylinder for an oblique incident wave is obtained by modifying the previous result for a normal wave to the form

$$p_t(a,\theta,z) = e^{ikz \sin \beta} \cdot \text{[Equation 10 with } k = k \cos \beta] \tag{23}$$

Clearly, the horizontal component of the force on a right circular surface element $2\pi\, a\, dz$ of the cylinder due to an oblique wave can utilize the results for a normally incident wave by just replacing k by k cos $\beta$ in Equations 14 and 15.

To obtain the net horizontal force over a finite length $\ell$ of the cylinder, due to an oblique wave, it is necessary to integrate over $\ell$. If the length $\ell$ is centered about the coordinate axes X, Z, then the net force is given by

$$F_t(\ell) = \text{[Equation 14 with } k = k \cos \beta] \cdot \int_{-\ell/2}^{+\ell/2} e^{ikz \sin \beta}\, dz$$

$$F_t(\ell) = \text{[Equation 14 with } k = k \cos \beta] \cdot \ell \cdot \left[ \frac{\sin\left(\frac{k\ell}{2} \sin \beta\right)}{\frac{k\ell}{2} \sin \beta} \right]$$

The acoustic force coupling factor for a finite length $\ell$ of the cylinder is the ratio of this force to the product of the incident pressure and normal area given by

$$L_t(\ell) = \frac{F_t(\ell)}{2\, P_0\, a\ell} = \frac{2}{(ka \cos \beta)\, C_1}\, e^{-i(\pi/2 + \gamma_1)}\, \frac{\sin\left(\frac{k\ell}{2} \sin \beta\right)}{\frac{k\ell}{2} \sin \beta} \tag{24}$$

This is the same as Equation 16 (when ka cos $\beta$ is substituted for ka directly and in the arguments for the functions $C_1$ and $\gamma_1$) multiplied by the additional sin x/x term. The latter term simply accounts for the average force over the length $\ell$ of the cylinder. For high frequencies, where $(k\ell/2) \sin \beta \gg 1$ and $ka \gg 1$, the upper envelope of the coupling factor will tend to

$$L_t(\ell) \simeq \sqrt{\frac{2\pi}{ka}} \cdot \frac{2}{k\ell \sin \beta} \tag{25}$$

3.0 ACOUSTIC FORCE ON A RIGID SPHERE IN A PLANE WAVE SOUND FIELD

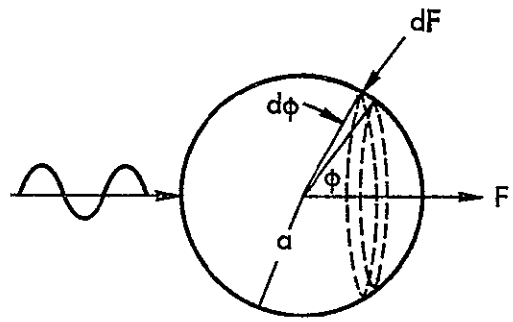


A plane progressive sound field incident on a sphere of radius a will exhibit circular symmetry about a polar axis through the sphere which is also the direction of the incident wave. Let $p(a,\phi)$ be the pressure on the surface of an elemental ring of radius $(a \sin \phi)$ and width $a\,d\phi$ where $\phi$ is the polar angle relative to the radius vector in the direction of the incident wave. The net radial force component will be (assuming a positive pressure corresponds to a radial force directed inward)

$$dF = p(a,\phi)\, 2\pi\, a \sin \phi \cdot a\, d\phi \tag{26}$$

If force is positive in the direction of propagation of the incident wave, the total force in the horizontal direction is

$$F = -2\pi a^2 \int_0^{\pi} p(a,\phi) \sin \phi \cos \phi \, d\phi \tag{27}$$

If the incident pressure at the center of the sphere is $P_0\, e^{-i\omega t}$, then the acoustic coupling factor for the sphere will be

$$L_i = \frac{F}{\pi a^2\, P_0\, e^{-i\omega t}} = -2 \int_0^{\pi} \frac{p(a,\phi)}{P_0\, e^{-i\omega t}} \sin \phi \cos \phi \, d\phi \tag{28}$$

3.1 Net Force on Sphere Without Considering Scattering

Consider first the net force without scattering. The incident pressure on the surface of the sphere can be defined by

$$p_i = P_0\, e^{-i(\omega t - ka \cos \phi)} = P_0\, e^{ika \cos \phi}\, e^{-i\omega t} \tag{29}$$

Substituting Equation 29 into Equation 28, the acoustic coupling factor for the incident field only is

$$L_i = -2 \int_0^{\pi} e^{ika \cos \phi} \sin \phi \cos \phi \, d\phi \qquad (30)$$

which reduces to

$$L_i = \frac{4}{ka} \left[ \frac{\sin ka}{ka} - \cos ka \right] e^{-i\pi/2} \qquad (31)$$

The limiting value at long wavelengths is obtained by using the first two series expansion terms in the above sine and cosine terms to give

$$L_i \simeq \frac{4}{3} ka \, e^{-i\pi/2}, \qquad ka << 1 \qquad (32)$$

## 3.2 Net Acoustic Force on Sphere Including Effect of Scattering

Using the same concept employed with the cylinder, the scattered field is determined by satisfying the boundary condition of zero radial velocity on the surface of the sphere. The solution for the incident and scattered pressure or total pressure on the sphere at the polar angle $\phi$ is the infinite series (Reference 1)*

$$p_t = \left[ P_0 \left( \frac{1}{ka} \right)^2 \sum_{m=0}^{\infty} \frac{(2m+1) \, e^{i\pi m/2}}{D_m \, e^{i\delta_m}} P_m (\cos \phi) \right] e^{-i\omega t} \qquad (33)$$

where

$$\left.\begin{aligned} &P_m(\cos \phi) = \text{Legendre Function of order m (Reference 1), and} \\ &P_0 (\cos \phi) = 1 \\ &P_1 (\cos \phi) = \cos \phi \\ &P_m(\cos \phi) = \frac{2m-1}{m} \cos \phi \, P_{m-1} (\cos \phi) - \frac{m-1}{m} P_{m-2} (\cos \phi) \end{aligned}\right\} \qquad (34)$$

The term $D_m \, e^{i\delta_m}$ is a complex function of ka and can be conveniently expressed in terms of complex Hankel functions as (References 1 and 2)

$$D_m \, e^{i\delta_m} = -i \sqrt{\frac{\pi}{2 \, ka}} \left[ \frac{m}{ka} H^1_{m+1/2} (ka) - H^1_{m+3/2} (ka) \right]. \qquad (35)$$

---

* The same result is obtained in page 363 of Reference 5 except for a change in sign convention by using +j instead of -i for $\sqrt{-1}$.

where

$H^1_{m+1/2}(z)$ = Bessel Function of third kind (or Hankel Function) and fractional order $m + 1/2$.

Asymptotic values of the amplitude $D_m$ and phase angle $\delta_m$ are given by Morse (Reference 1) as follows:

$$D_m \simeq \begin{cases} (1/ka)^2 & m = 0,\ ka \ll 1/2 \\ \dfrac{1 \cdot 3 \cdot 5 \cdot \ \ldots (2m-1)\,(m+1)}{(ka)^{m+2}} & m > 0,\ ka \ll m+1/2 \\ 1/ka & m \geq 0,\ ka \gg m+1/2 \end{cases} \tag{36}$$

$$\delta_m \simeq \begin{cases} \dfrac{1}{3} ka & m = 0,\ ka \ll 1/2 \\ \dfrac{m\,(ka)^{2m+1}}{1 \cdot 3 \cdot 5 \cdot \ \ldots (2m-1)^2\,(2m+1)(m+1)} & m > 0,\ ka \ll m+1/2 \\ ka - \dfrac{1}{2}\pi\,(m+1) & m \geq 0,\ ka \gg m+1/2 \end{cases} \tag{37}$$

Tabulated values of $P_m(\cos\phi)$, $D_m$, and $\delta_m$ have been published (References 1 and 2) and graphical representation of Equation 33 has been presented by Weiner (Reference 4) and Morse (Reference 1). An approximate value for the pressure at any point $(a, \phi)$ for long wavelengths is obtained by using only the first two terms of Equation 33. The result is

$$p_t \simeq P_0 \left[1 + i\,\frac{3}{2}\,ka \cos\phi\right] e^{-i\omega t}, \quad ka \ll 1 \tag{38}$$

The incident pressure for long wavelengths can be expressed, from Equation 29, as

$$p_i \simeq P_0 \ [1 + ika \cos\phi]\ e^{-i\omega t}, \quad ka \ll 1, \tag{39}$$

so that for low frequencies, the scattered pressure at the surface of the sphere is just 1/2 the quadrature component of the incident pressure which varies with $\phi$.

To define the acoustic coupling factor, including scattering, we substitute the term in brackets in Equation 33 into Equation 28 and carry out the required integration. This involves integration of terms of the form

$$\int_0^{\pi} P_m (\cos \phi) \sin \phi \cos \phi \, d\phi$$

Due to the orthogonality property of Legendre functions (Reference 2), it can be shown that only the term for m = 1 has a non-zero integral and this is equal to 2/3. Thus, the acoustic coupling factor can be expressed in closed form using Equations 28, 33 and 36 as

$$L_t = \frac{4\sqrt{2/\pi \; ka}}{H^1_{3/2}(ka) - ka\, H^1_{5/2}(ka)} \tag{40}$$

Equation 40 is the result obtained by Weiner which is cited in Reference 6.

Since the quantities $D_1$ and $\delta_1$ are tabulated in Morse (Reference 1), it is also convenient to use Equation 33 directly in Equation 28 to give the following simple but exact expression for the acoustic force coupling factor for a rigid sphere:

$$L_t = \left(\frac{2}{ka}\right)^2 \frac{e^{-i(\pi/2 + \delta_1)}}{D_1} \tag{41}$$

However, a much simpler form for this expression is possible by utilizing algebraic and trigonometric expressions for $D_1$ and $\delta_1$ in terms of ka, which are derived in Appendix A.

It is shown that the acoustic force coupling factor can be expressed in a closed form as

$$L_t = \frac{4\, ka}{\sqrt{4 + (ka)^4}}\, e^{-i(ka + \alpha - \pi/2)} \tag{42}$$

where

$$\alpha = \tan^{-1} \frac{2\, ka}{(ka)^2 - 2}$$

Thus, Equations 40 - 42 provide three equivalent expressions for the net force on a rigid sphere. The magnitude and phase angle of $L_t$ for a sphere have been plotted in Figures 6 and 7. The approximation given by Equation 31, which defined the net load without considering scattering, is also shown in Figure 6. The maximum acoustic force is just twice the incident pressure times normal area and occurs when the wavelength

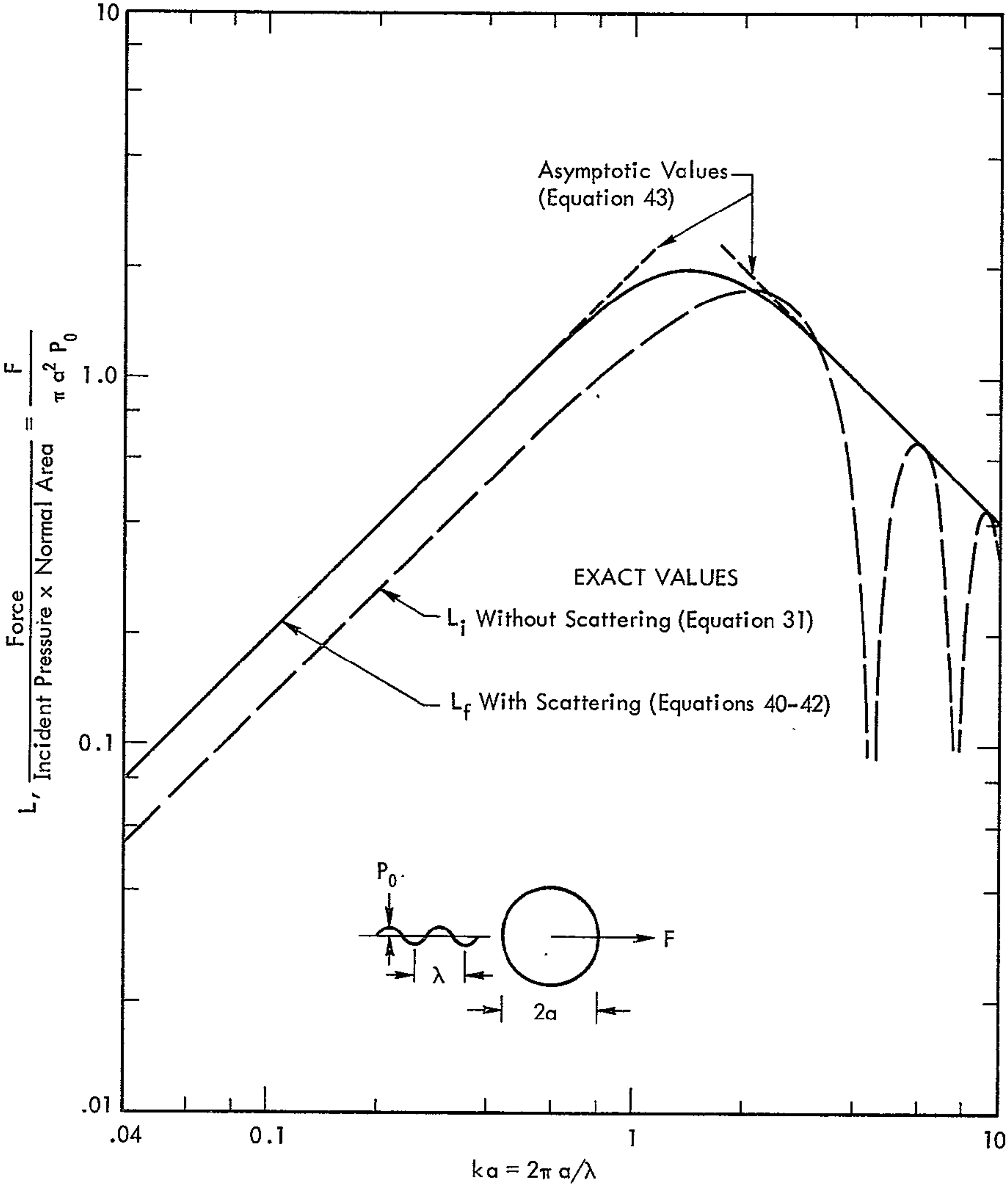


Figure 6. Acoustic Force Coupling Factor for Rigid Sphere In Plane Wave Sound Field

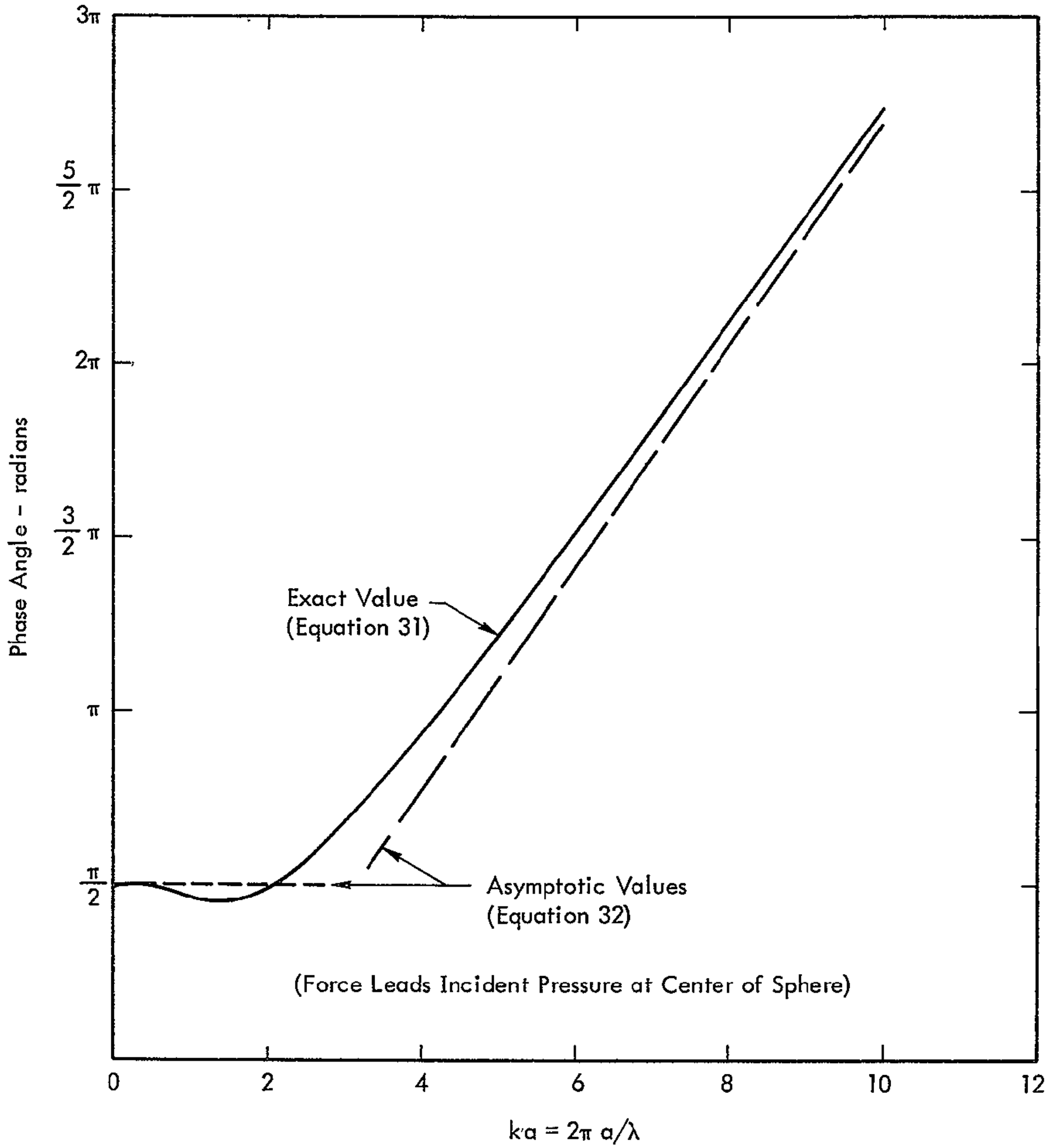


Figure 7. Phase Angle Between Acoustic Force on Sphere and Normally Incident Plane Wave Referred to Center of Sphere

is equal to $2\pi a/\sqrt{2}$ or $ka = \sqrt{2}$ instead of $ka = 1$ as for the cylinder. Again, note that for large values of ka, as for the cylinder, the envelope of the net force, neglecting scattering, is approximately the same as the true force, including scattering.

As shown in Figure 7, the force leads the incident pressure referred to the center of the sphere. The phase angle approaches $\pi/2$ for long wavelengths and then increases rapidly for $ka > 2$.

Limiting values for $L_t$ can be easily derived from Equation 41 or 42 and are given by

$$\left.\begin{aligned} L_t &\simeq 2\,ka\, e^{-i\pi/2}, && ka \ll 1 \\ \text{and} \quad L_t &\simeq \frac{4}{ka}\, e^{-i(ka - \pi/2)}, && ka \gg 1 \end{aligned}\right\} \tag{43}$$

These approximations are also shown in Figure 6.

Comparing Equation 43 with the approximation for long wavelengths without scattering in Equation 32, it is seen that at long wavelengths, the amplitude of the true acoustic force is 3/2 times the value predicted by the incident field only. This agrees with the previous conclusion that for long wavelengths, the scattered field adds 50 percent to the quadrature component of the incident field to make up the total pressure on the sphere. Since the magnitude of this component is dependent on angular position around the sphere, it is the source of the unbalanced pressure distribution, and, hence, net force on the sphere.

## 4.0 MOTION OF OBSTACLES IN A PLANE WAVE FIELD

The discussion so far has been concerned solely with the acoustic force on rigid obstacles in a plane wave field. The motion of the obstacle resulting from this force will be considered in the following. It is first necessary, however, to account for the interaction between the incident field and the radiation of the moving obstacle in this field. The basic principle is that the driving force on the moving obstacle can be considered the same as the force on the rigid obstacle providing radiation loading due to motion of the obstacle is properly accounted for.

### Forced Motion of a Sphere, Including Radiation Reaction Forces

As a first approach to the problem, consider the motion of a sphere of radius a under excitation by a mechanical harmonic radial force, $F = F_0\, e^{-i\omega t}$. Assume that the sphere is supported by a damped spring system as illustrated in the following sketch

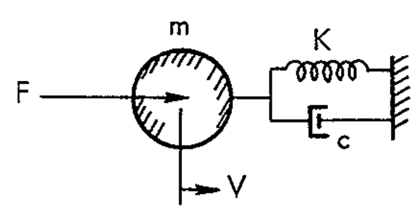


The equation for the resulting harmonic motion of the sphere in a vacuum can be expressed as

$$F = F_0\, e^{-i\omega t} = V_0 Z_m\, e^{-i\omega t} \tag{44}$$

where $Z_m$ is the mechanical impedance of the supported sphere given by

$$Z_m = c - i\omega m + i\, K/\omega$$

and

$c$ = damping constant of support

$m$ = mass of sphere

$K$ = spring constant

$V_0$ = velocity amplitude.

The motion of the sphere in air results in sound radiation. The reaction force back on the sphere due to radiation opposes the driving force and may be accounted for by the addition of a radiation impedance to the system. Viscous forces are neglected for now. Thus, in air, the equation of motion of the sphere is modified to become

$$F = F_0 \, e^{-i\omega t} = V_0 (Z_m + Z_a) \, e^{-i\omega t} \tag{45}$$

where $Z_a$ is the radiation impedance and $VZ_a$ is the reaction force due to radiation which opposes the driving force. The radiation impedances for oscillating and pulsating spheres and cylinders are reviewed in detail in Appendix B. For the oscillating sphere, the radiation impedance is given by

$$Z_a = \frac{4}{3} \pi a^2 \rho c \left[ \frac{(ka)^4 - i\,(2ka + (ka)^3)}{4 + (ka)^4} \right] \tag{46}$$

where

$\rho c$ = radiation resistance of air

$ka$ = $\omega a / c$ = nondimensional frequency

The resistive and reactive components of this impedance divided by $\pi a^2 \rho c$ (i.e., the product of the normal area of the sphere and the acoustic resistance of air) are shown in Figure 8.

The motion of the sphere in a plane wave sound field is determined by the same approach. The mechanical driving force F, in Equation 45, can be replaced by an acoustic force equal to the net summation of the incident plus scattered pressure field. This approach can be applied to any other obstacle or structure which can be vibrated by an incident acoustic field. In other words, the motion of an obstacle in a sound field can be described by treating the driving force as the force on the rigid obstacle. The total impedance opposing the driving force is the sum of the mechanical impedance $Z_m$ of the obstacle and its support plus the radiation impedance $Z_a$ of the body. Thus, a general expression for the velocity amplitude of a structure in a plane wave sound field is given by

$$V = \frac{P_0 A_n L_t}{Z_m + Z_a} \tag{47}$$

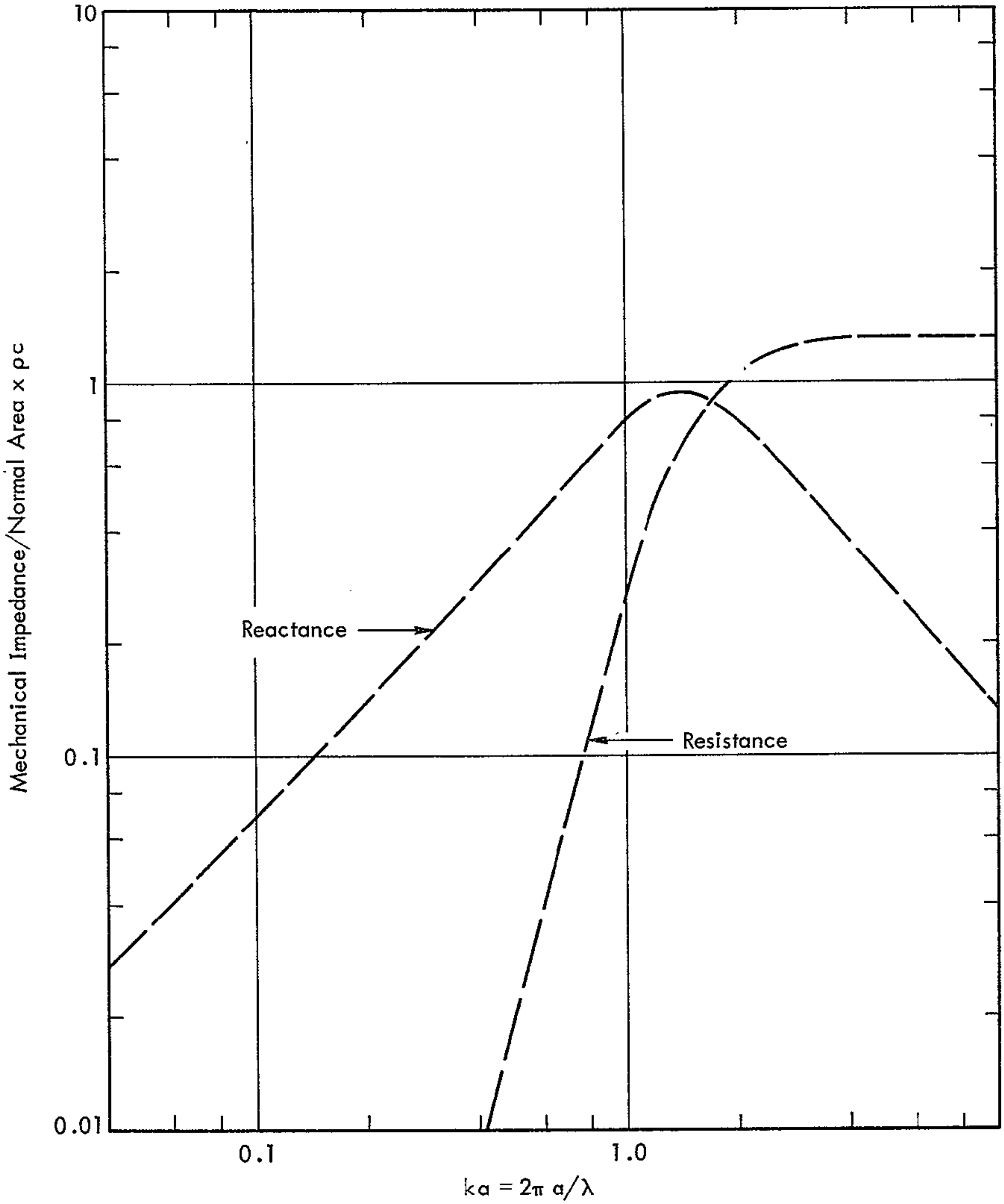


Figure 8. Radiation Impedance of an Oscillating Sphere

where

$P_0$ = amplitude of incident sound pressure

$A_n$ = projected area of structure normal to incident sound wave (e.g., $\pi a^2$ for sphere)

$L_f$ = acoustic force coupling constant (e.g., Equation 42 for sphere)

It should be clearly pointed out that the observed sound pressure at the surface of an obstacle or structure which is moving due to excitation by an incident field will, in general, be different from the pressure predicted for a rigid structure. However, this difference will be significant only near resonance frequencies of the structure and then only when it has a relatively low mass density and/or very low damping.

## 5.0 EXPERIMENTAL DATA ON RESPONSE OF UNBAFFLED OBSTACLES IN A PLANE WAVE SOUND FIELD

As an illustration of the preceding theory, two examples of measured vibration of unbaffled obstacles in a sound field are considered. The first case represents data obtained by von Bekesy on the vibration of the head in a plane wave sound field (Reference 8). For excitation by a sound pressure level of 134 dB at discrete frequencies, the measured acceleration amplitude A of the head over a frequency range of 100 to 500 Hz was closely described by the simple expression,

$$A \simeq 2 \times 10^{-4} \ f, \quad g's \tag{48}$$

where f = frequency in Hz.

Since the head decouples, dynamically, from the neck at frequencies above about 2 to 10 Hz and has no structural resonances below 500 Hz (Reference 9), it may be considered as essentially a free mass, approximating a rigid sphere, in the frequency range of 100-500 Hz.

For an average radius of 3.75 in. and a weight of 7.5 lb, the expected acceleration amplitude can be estimated by applying Equation 43 for the case $ka << 1$. (Over the range of 100-500 Hz, $ka = \omega a/c = 0.15$ to $0.75$.) The resulting estimated acceleration is

$$A \simeq 2.8 \times 10^{-4} \ f, \quad g's \tag{49}$$

Thus, for this rather unusual case, the basic theory for the force on a rigid sphere provides a very close estimate of the motion of the head in a plane wave sound field

Another example is provided by data reported by Noiseux on the relative vibration response of a 2 x 10 x 1/16-inch aluminum plate, with and without a baffle, under excitation by plane waves over the frequency range of 90 to 250 Hz (Reference 10) To a first approximation, it can be expected that the acoustic force coupling factor for an infinite cylinder, relative to a maximum value of $\sim 2$ for a baffled cylinder, should provide a reasonable estimate of the relative vibration response in this case. Such an approach is illustrated in Figure 9. This shows that the theory for net force on an infinite cylinder does indeed provide a reasonable estimate for the relative influence of a baffle on vibration response of a long thin plate.

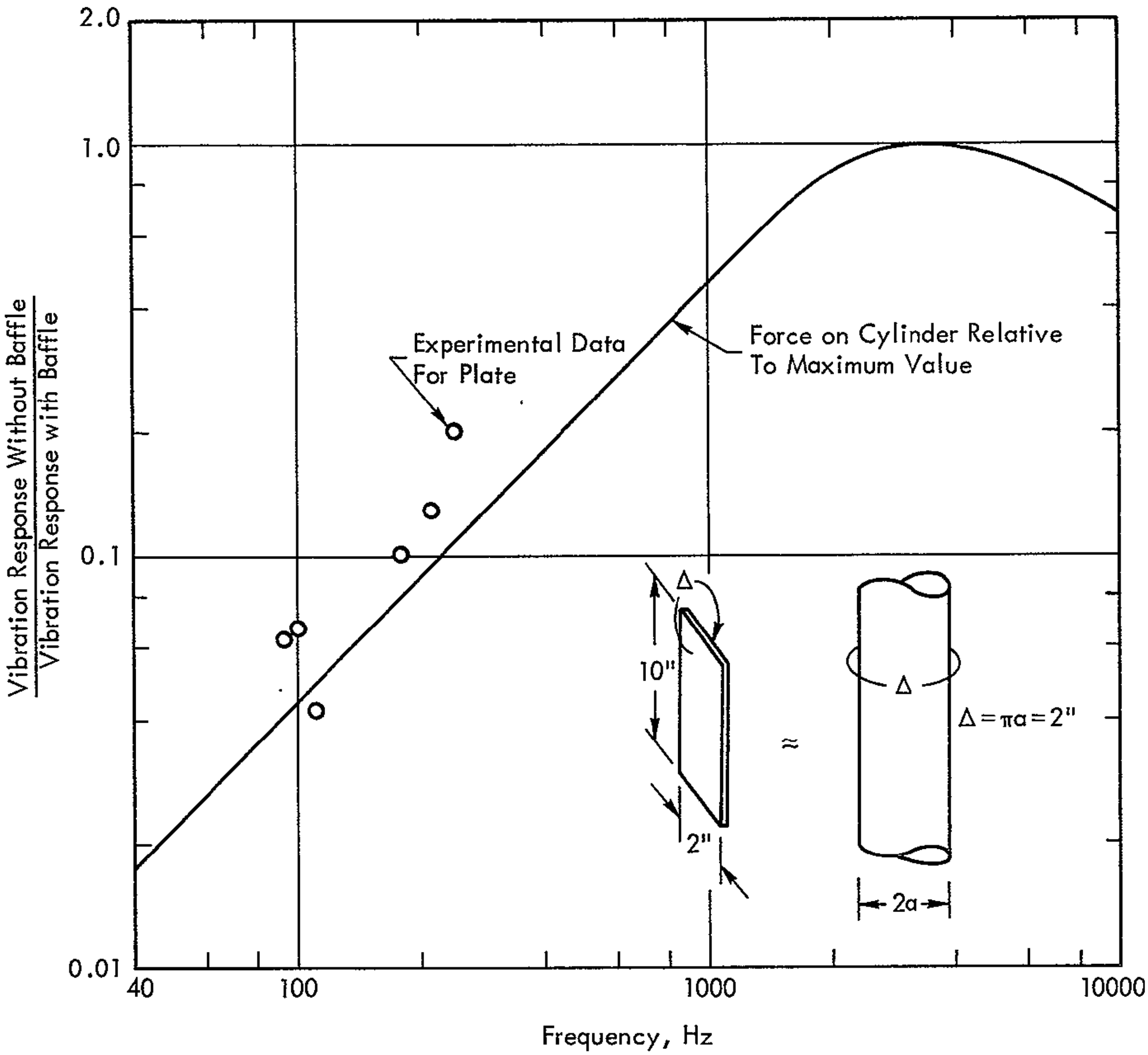


Figure 9. Comparison of Relative Vibration Response of Baffled and Unbaffled Long Panel with Theoretical Estimate Based on Net Force on Infinite Cylinder (Data From Reference 10)

## 6.0 VISCOUS FORCES ON OSCILLATING OBSTACLES

A unique set of experimental data were reported by Stephens and Scavullo on viscous damping of various types of oscillating bodies (Reference 11). For spheres and long cylinders, the data were generally in very close agreement with theory on viscous forces on such oscillating bodies. Data observed for vibrating plates or beams were also obtained and were collapsed by a simple empirical expression applicable for small amplitude oscillations. The theoretical or empirical expressions confirmed by these data are reviewed here.

### Oscillating Spheres

The dynamic viscous force acting on a sphere undergoing small amplitude pendulum oscillations in an incompressible viscous fluid has been studied theoretically by Lamb (Reference 12). Such oscillations can be considered equivalent to small amplitude linear oscillations. The viscous drag force can therefore be treated as equivalent to a mechanical resistance or ratio of damping force to linear translation velocity of the sphere. The resulting expression is

$$R_v = 3\pi \rho a^3 \omega \left[ \frac{1}{a} \left( \frac{2\nu}{\omega} \right)^{\frac{1}{2}} + \frac{1}{a^2} \left( \frac{2\nu}{\omega} \right) \right] \tag{50}$$

where

$a$ = radius of sphere

$\rho$ = mass density of viscous fluid surrounding sphere

$\omega$ = frequency, radians/sec

$\nu$ = kinematic viscosity.

It is useful to compare this viscous drag resistance with the mechanical radiation resistance $R_a$ for an oscillating sphere. From Equation 46, the latter can be expressed in the dimensionless form

$$\frac{R_a}{\pi a^2 \rho c} = \frac{4}{3} \left[ \frac{(\omega a/c)^4}{4 + (\omega a/c)^4} \right] \tag{51}$$

where $c$ = speed of sound.

If a new dimensionless variable $\sqrt{2\nu/ac}$ is defined, the viscous drag resistance $R_V$ can be also expressed in a similar form as

$$\frac{R_V}{\pi a^2 \rho c} = 3\left[\left(\frac{\omega a}{c}\right)^{\frac{1}{2}}\left(\frac{2\nu}{ac}\right)^{\frac{1}{2}} + \left(\frac{2\nu}{ac}\right)\right] \tag{52}$$

For air at sea level pressure and 68°F,

$$\nu = 0.0234 \text{ in.}^2/\text{sec}$$

$$c = 13{,}440 \text{ in./sec}$$

so that for these conditions

$$\frac{2\nu}{ac} = 3.48 \times 10^{-6}/a$$

where $a$ = radius of sphere in inches.

Equations 51 and 52 are compared in Figure 10 as a function of the dimensionless frequency $\omega a/c$. The radius of the sphere, $a$, is a parameter for the nondimensional viscous resistance defined by Equation 52. The plot shows the true variation with frequency for either form of resistance. However, variation of the viscous damping resistance with radius of the sphere is not clearly indicated in Figure 10. In fact, the nondimensional value of this resistance, $R_V/\pi a^2 \rho c$, is nearly independent of radius $a$ for $a > 0.1$ inch. The experimental verification of the theory for viscous damping, reported in Reference 11, covered only a single value of the parameter $\omega a/c$ ($= 0.0055$) for a 3.09-inch radius sphere. This is well outside the range where acoustic radiation resistance is significant.

Oscillating Cylinder

The theory of viscous damping of an infinite cylinder oscillating at right angles to its axis has been presented by Stokes (Reference 13). When expressed in the same normalized form used for the oscillating sphere, the viscous drag resistance, divided by the normal area per length $\ell$, times the specific acoustic reistance $\rho c$, is

$$\frac{R_V}{(2a\ell)\cdot \rho c} = \pi\left[2\left(\frac{\omega a}{c}\right)^{\frac{1}{2}}\left(\frac{2\nu}{ac}\right)^{\frac{1}{2}} + \left(\frac{2\nu}{ac}\right)\right] \tag{53}$$

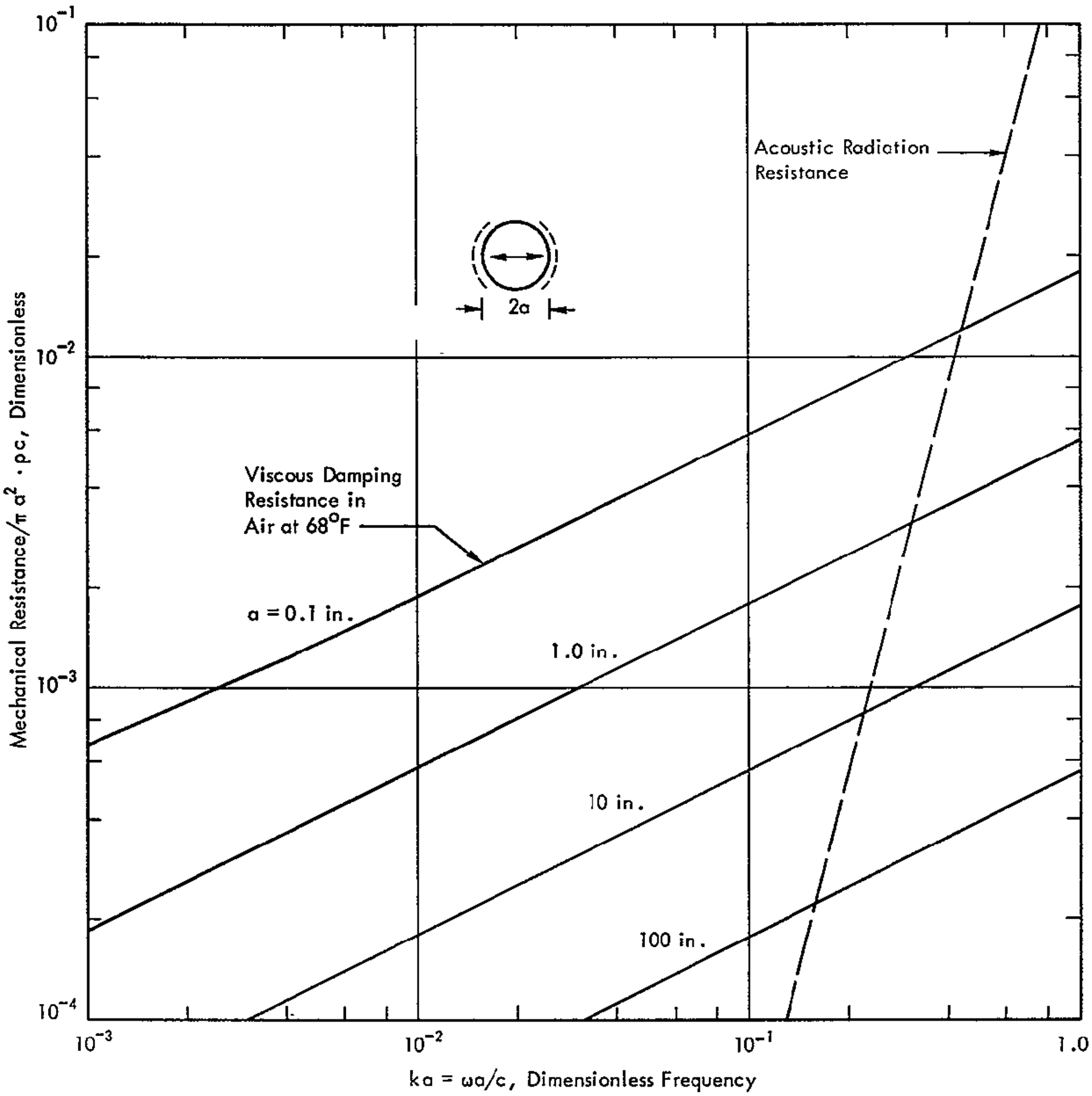


Figure 10. Comparison of Normalized Mechanical Resistance for Acoustic Radiation and Viscous Damping of Oscillating Solid Sphere; $\pi a^2$ = Normal Area, $\rho$ = Air Density, c = Speed of Sound

where

$a$ = radius of cylinder

$\ell$ = length of cylinder ($\gg a$)

and the other parameters are the same as defined earlier. (Note that $R_V$ is actually independent of the velocity of sound, c; this parameter only appears due to the particular normalized form used for convenience to allow comparison with the acoustic resistance.)

Comparing Equation 53 with Equation 52, it is clear that for the same normal area for the sphere or cylinder, the viscous drag resistance for the latter is roughly twice as great ($\sim 2\pi/3$) as for the sphere. (The second term inside the brackets in each expression is normally insignificant.)

The acoustic radiation resistance $R_a$ of an oscillating cylinder is given in Appendix B. For small values of the frequency parameter, $ka = \omega a/c$, this resistance, expressed in the same normalized form, is approximately equal to (see Equation B-16, Appendix B)

$$\frac{R_a}{(2a\ell)\cdot\rho c} \simeq \frac{\pi^2}{4}\,(\omega a/c)^3\,, \quad \omega a/c < 1 \tag{54}$$

Equations 53 and 54 are compared in Figure 11 and show, as for the sphere, that viscous damping resistance is much greater than the acoustic radiation resistance only for small values of $\omega a/c$. The experimental data on viscous damping of cylinders in air, cited in Reference 11 was obtained in the range of $\omega a/c$ where acoustic radiation damping was negligible. Providing the peak amplitude of oscillation was small relative to the cylinder radius, the experimental value of viscous damping resistance agreed with the value predicted by Equation 53. At higher amplitudes, the damping resistance increased due, apparently, to flow separation or end effects (Reference 11).

## Oscillating Plates

The data on damping of oscillating unbaffled plates reported in Reference 11 exhibited a consistent but nonlinear behavior. Linear viscous damping theory was not applicable. The observed data can be defined in terms of an empirical expression for an equivalent damping resistance as

$$R_d = 2\,K\,\rho\,V\,A^{4/3} \tag{55}$$

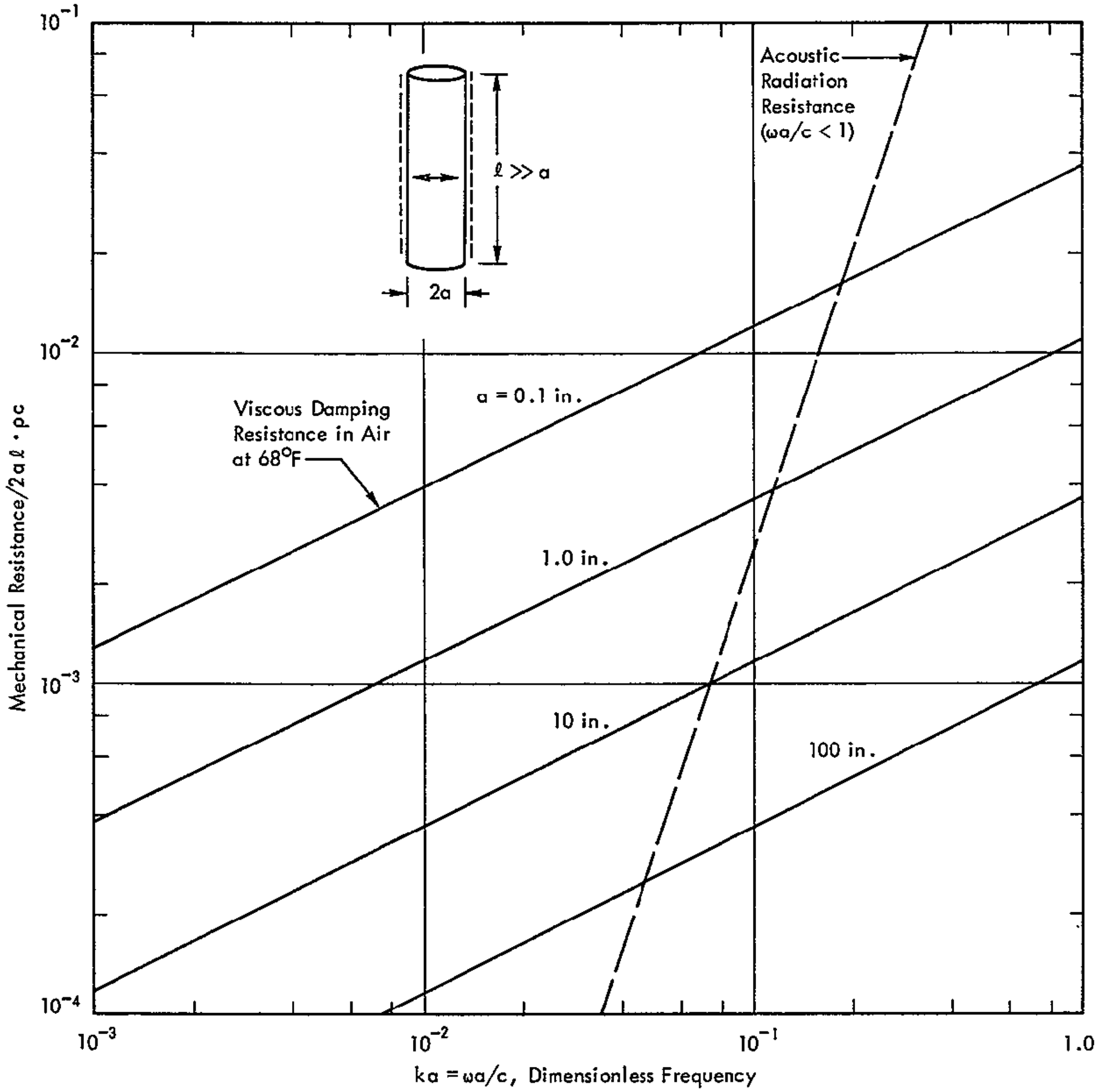


Figure 11. Comparison of Normalized Mechanical Resistance for Acoustic Radiation ($\omega a/c < 1$) and Viscous Damping Resistance of Oscillating Right Circular Cylinder with Length ($\ell$) >> Radius ($a$)

where

$\rho$ = mass density of air

$V$ = velocity amplitude

$A_n$ = area of panel

$$K = \begin{cases} \text{empirical constant} \\ \text{22 for ft, lb, sec units or} \\ \text{4.2 for in., lb, sec units} \end{cases}$$

This expression was derived in Reference 11 from the experimental results and corresponding empirical collapse of data. The data were obtained for thin rectangular and circular plates with areas ranging from 15 to 220 in.$^2$ oscillated at a frequency of 3.8 Hz and 21.2 Hz. For displacements greater than 0.1 inch, the damping resistance is closely predicted by Equation 55 in all cases.

The nonlinear nature of this damping resistance indicates that the damping force is aerodynamic in origin; i.e., it is proportional to $\rho V^2$ (Reference 11). For comparison to this nonlinear resistance, the linear acoustic radiation resistance load at low frequencies, on an oscillating circular piston in free space (without a baffle), is given approximately by (Reference 14)

$$R_a \simeq .056\,\pi a^2 \rho c \cdot \left(\frac{\omega a}{c}\right)^4, \qquad \omega a/c < 1 \tag{56}$$

For comparison of the absolute values of the two resistances defined by Equations 55 and 56, consider the case of a circular plate with the following constants:

| | | | |
|---|---|---|---|
| Area | $A_n$ | = | 220 in.$^2$ |
| Radius | $a$ | = | 8.38 in. |
| Frequency | $\omega/2\pi$ | = | 21.2 Hz |
| Velocity Amplitude | $V$ | = | 13.3 in./sec ($\pm$ 0.1 in. at 21.2 Hz) |
| Mass Density | $\rho$ | = | $0.112 \times 10^{-6}$ lb sec$^2$/in.$^4$ at 68$^\circ$F |
| Specific Acoustic Resistance | $\rho c$ | $\simeq$ | 0.0015 lb sec/in.$^3$ at 68$^\circ$F |

From Equation 55, the aerodynamic "resistance" is

$$R_d = 1.66 \times 10^{-2} \text{ lb sec/in.}$$

From Equation 56, the acoustic radiation resistance for this case would be

$$R_a = 0.88 \times 10^{-6} \text{ lb sec/in.}$$

Clearly, the aerodynamic damping resistance exceeds the acoustic radiation resistance for this case

A general comparison of the relative value of these two resistances which oppose the motion of oscillating, rigid, thin plates is not practical. However, in any studies involving such motion, it seems clear from these limited results that the aerodynamic resistance is likely to be much more significant than the acoustic radiation resistance for small values of the frequency parameter $\omega a/c$

## 7.0 CONCLUSIONS

The theory for forces acting on stationary spheres and cylinders in a plane wave sound field has been reviewed in a consistent manner to illustrate the following points:

- The total acoustic force on solid spheres and cylinders for wavelengths much greater than the circumference is 2 times and 1.5 times, respectively, the incident "force" ( incident pressure times normal area). At these frequencies, the force leads the incident pressure at the center of the obstacle by approximately 90 degrees.

- At high frequencies, where the incident wavelength is small relative to the circumference of the obstacle, the upper envelope of the incident force is very nearly the same as the true net force, including scattering effects.

- The net force on a cylinder in a plane wave field arriving at an oblique angle to the cylinder axis is predicted by a simple modification of the usual expression for the force in a normally incident field. This modification amounts to accounting for the effective incident wavelength at right angles to the cylinder and the trace wavelength along the cylinder.

- Simplified expressions for the total net force on obstacles can be derived which accurately describe the true net force at long wavelengths.

Theory and data on forces acting on oscillating solid obstacles are also covered.

- The motion of an obstacle in a sound field is determined by first defining the force on a rigid obstacle and then adding an acoustic radiation impedance term to the mechanical motional impedance of obstacle. This is a general result applicable to any case of acoustic loading of structure.

- In addition to acoustic radiation forces acting on solid oscillating obstacles, such as spheres, cylinders or plates, viscous damping forces also are effective. The latter predominate for radiation wavelengths large relative to the obstacle circumference. For oscillating thin plates, the viscous damping forces become nonlinear for oscillation amplitudes comparable to the plate thickness. The nonlinearity indicates that the damping force is aerodynamic in origin and is thus proportional to $\rho V^2$ instead of directly proportional to V as for acoustic or linear viscous forces.

- Limited experimental data are cited which are in agreement with these observations.

## REFERENCES


1. P. M. Morse, "Vibration and Sound," McGraw-Hill Book Co., New York (1948).

2. M. Abramowitz and I. A. Stegun, "Handbook of Mathematical Functions," National Bureau of Standards (June 1964).

3. R. B. Lindsay, "Mechanical Radiation," McGraw-Hill Book Co., New York (1960).

4. F. M. Weiner, "Sound Diffraction by Rigid Spheres and Circular Cylinders," J. Acoust. Soc. Am. 19 444 (1947).

5. S. N. Rischevkin, "A Course of Lectures on the Theory of Sound," Pergamon Press, The MacMillan Co., New York (1963).

6. J. Zwislocki, "In Search of the Bone Conduction Threshold in a Free Sound Field," J. Acoust. Soc. Am. 29 795 (1957).

7. A. Wenzel, "Surface Pressure Correlation Function for a Cylinder in a Diffuse Reverberant Sound Field," Wyle Laboratories Research Staff Report WR 66-16 (March 1966).

8. G. von Bekésy, Chapter 7, "Handbook of Experimental Psychology," S. S. Stevens (ed.), John Wiley and Sons, New York (1962).

9. H. E. von Gierke, "Biodynamic Response of the Human Body," Appl. Mech. Rev. 17, pp. 951-958 (December 1964).

10. D. U. Noiseux, "Response of Electronics to Intense Sound Fields," WADD TR 60-754 (January 1961).

11. D. A. Stephens and M. A. Scavullo, "Effect of Pressure Environment on Damping of Vibrating Structures," Shock and Vibration Bulletin, No. 34 (1964).

12. H. Lamb, "Hydrodynamics," Sixth Edition, Dover Publications, New York (1945)

13. G. G. Stokes, Cambridge Philosophical Soc. Trans., Vol. 9, pp. 8-106 (1851)

14. H. F. Olson, "Acoustical Engineering," D. Van Nostrand Co., New York (1957)

## APPENDIX A

## SIMPLIFIED EXPRESSION FOR NET FORCE ON A SPHERE

Based on Morse's theory (Reference 1), Equation 41 specifies the acoustic force coupling factor for a rigid sphere in a plane wave sound field as

$$L_t = \left(\frac{2}{ka}\right)^2 \frac{e^{-i(\pi/2+\delta_1)}}{D_1} \qquad \text{(A-1)}$$

where

$k$ = wave number of incident field

$a$ = radius of sphere

$D_1, \delta_1$ = functions of $ka$ defined by Equation 35 for $m = 1$.

The coupling factor $L_t$ is the ratio of net acoustic force to the product of the incident pressure at the center of the sphere and the normal area. A more convenient expression for $L_t$ is developed below based on an extension of the derivation for the force on a sphere in Reference 5. Equation A-1 may be expressed as

$$L_t = \left(\frac{2}{ka}\right)^2 \frac{1}{D_1}\,[-\sin\delta_1 - i\cos\delta_1] \qquad \text{(A-2)}$$

From Morse (Reference 1), the definition for $D_1$ and $\delta_1$ can also be expressed as the differential:

$$D_1\,e^{i\delta_1} = -i\,\frac{d}{d(ka)}\,[j_1(ka) + i\,y_1(ka)] \qquad \text{(A-3)}$$

where $j_1(ka)$ and $y_1(ka)$ are spherical Bessel Functions of the first and second kind, respectively. These Bessel Functions have the following properties (References 1, 2 and 5)

$$\frac{d}{dz}\,[j_m(z)] = \frac{1}{2m+1}\,[m\,j_{m-1}(z) - (m+1)\,j_{m+1}(z)] \qquad \text{(A-4)}$$

where $j_m(z)$ represents either of the spherical Bessel Functions in Equation A-3 for $m = 1$ and $z = ka$.

In addition, the following transformations are known (References 1 and 2)

$$j_0(z) = \frac{\sin z}{z} \; , \; y_0(z) = -\frac{\cos z}{z}$$

$$j_2(z) = \left(\frac{3}{z^3} - \frac{1}{z}\right) \sin z - \frac{3}{z^2} \cos z \tag{A-5}$$

$$y_2(z) = -\frac{3}{z^2} \sin z - \left(\frac{3}{z^3} - \frac{1}{z}\right) \cos z$$

Utilizing Equations A-2 to A-5, it can be shown that:

$$D_1 \cos \delta_1 = \frac{1}{3} [y_0(ka) - 2\, y_2(ka)]$$

$$D_1 \sin \delta_1 = -\frac{1}{3} [j_0(ka) - 2\, j_2(ka)]$$

$$D_1 = \sqrt{4 + (ka)^4}/(ka)^3$$

$$\cos \delta_1 = -\cos (ka + \alpha)$$

and

$$\sin \delta_1 = -\sin (ka + \alpha)$$

where

$$\alpha = \tan^{-1} 2\, ka/[(ka)^2 - 2]$$

With these relationships, Equation A-2 can be expressed in closed form as

$$L_t = \frac{4ka}{\sqrt{4 + (ka)^4}} e^{-i\,(ka + \alpha - \pi/2)} \tag{A-6}$$

which is the same as Equation 42 in the text.

## APPENDIX B

## RADIATION IMPEDANCE OF OSCILLATING AND PULSATING SPHERES AND CYLINDERS

### OSCILLATING SPHERE

The radiation from an oscillating rigid sphere is ordinarily treated by considering the oscillating sphere as a dipole source (References 1 and 5). A somewhat more general but equivalent approach is used here by assuming only that a spherical wave is radiated from the sphere. The boundary condition requires that the radial component of the motion of the sphere is equal to the radial component of particle velocity of the radiated spherical wave.

Assume a sphere of radius $a$, oscillating along a polar axis with a velocity $V\, e^{-i\omega t}$, radiates a spherical pressure field with polar symmetry which can be defined by the infinite series of spherical waves (References 1 and 5)

$$p(r,\phi) = \sum_{m=0}^{\infty} a_m\, P_m(\cos\phi)\, h'_m(kr)\, e^{-i\omega t} \tag{B-1}$$

where $p(r,\phi)$ = instantaneous pressure at a point $r,\phi$ (in spherical coordinates)

$P_m(\cos\phi)$ = Legendre Function of order m

$h'_m(kr)$ = spherical Bessel Function of the third kind

and

$a_m$ = a constant to be defined.

The radial particle velocity at the surface of the sphere ($r=a$) is

$$u_n(a,\phi) = \frac{1}{i\omega\rho}\frac{\partial p}{\partial r}\bigg|_{r=a} = \frac{k}{i\omega\rho}\frac{\partial p}{\partial(kr)}\bigg|_{r=a} \tag{B-2}$$

This must equal the radial component of velocity of the sphere, $V(\cos\phi)\, e^{-i\omega t}$ where $\phi$ is the polar angle. Thus, satisfying the boundary condition, and using Equation 34 from the main body of the text,

$$V\cos\phi\, e^{-i\omega t} = \frac{k}{i\omega\rho}\, e^{-i\omega t}\sum_{m=0}^{\infty} i\, a_m\, P_m(\cos\phi)\, D_m(ka)\, e^{i\delta_m(ka)} \tag{B-3}$$

where

$$i\, D_m(ka)\, e^{i\,\delta_m(ka)} = \frac{d}{d(kr)}\,[h'_m(kr)]_{r=a}$$

The left side of Equation B-3 has only one cosine term. For the right side, since $P_m(\cos\phi) = \cos\phi$ only for $m = 1$, all the other terms drop out and we can solve for the constant $a_1$.

$$a_1 = \frac{\rho c\, V e^{-i\,\delta_1(ka)}}{D_1(ka)} \qquad \text{(B-4)}$$

Thus, the pressure at the surface of the sphere is given by

$$p(a,\phi) = \frac{\rho c\, V \cos\phi\, e^{-i\,\delta_1(ka)}\, h'_1(ka)\, e^{-i\omega t}}{D_1(ka)} \qquad \text{(B-5)}$$

By using the following transformations (References 1, 2 and 5) (see Appendix A)

$$D_1(ka) = \sqrt{4 + (ka)^4}/(ka)^3$$

$$h'_1(ka) = \frac{\sin ka}{(ka)^2} - \frac{\cos ka}{ka} - i\left[\frac{\sin ka}{ka} + \frac{\cos ka}{(ka)^2}\right]$$

$$\delta_1(ka) = ka + \tan^{-1}\left[\frac{2\,ka}{(ka)^2 - 2}\right] \pm \pi\,,$$

Equation B-5 can be reduced to the following expression for the pressure on the surface of an oscillating sphere

$$p(a,\phi) = \rho c\, V \cos\phi \left[\frac{(ka)^4 - i\,(2\,ka + (ka)^3)}{4 + (ka)^4}\right] e^{-i\omega t} \qquad \text{(B-6)}$$

which is identical to the expression derived in Reference 5 by treating the oscillating sphere as a dipole*.

---

* Note, again, the convention of using $-i$ instead of $+j$ for this report.

The reaction force back on the sphere due to this radiation is in the direction of motion and is found by the integral (see Equation 27)

$$F_r = - \quad 2\pi a^2 \int_0^{\pi} p(a, \phi) \sin \phi \cos \phi \, d\phi \tag{B-7}$$

Substituting Equation B-6 in the above, the reaction force is found to be

$$F_r = - V \left\{ \frac{4}{3} \pi a^2 \rho c \left[ \frac{(ka)^4 - i(2\,ka + (ka)^3)}{4 + (ka)^4} \right] \right\} e^{-i\omega t} \tag{B-8}$$

The equal and opposite driving force necessary to overcome this radiation reaction, when divided by the velocity of the sphere $Ve^{-i\omega t}$, is called the mechanical radiation impedance, $Z_a$, of the oscillating sphere. This is equal to the term in curly brackets above.

$$Z_a = \frac{4}{3} \pi a^2 \rho c \left[ \frac{(ka)^4 - i(2\,ka + (ka)^3)}{4 + (ka)^4} \right] \tag{B-9}$$

Note that for long wavelengths (ka << 1)

$$Z_a \simeq 4\pi a^2 \rho c \left[ \frac{(ka)^4}{12} - i \frac{ka}{6} \right]$$

or

$$Z_a \simeq 4\pi a^2 \rho c \frac{(ka)^4}{12} - i \frac{\omega M_s}{2}, \quad ka << 1 \tag{B-10}$$

where $M_s = (4/3 \, \pi a^3 \rho)$.

Thus, the radiation impedance, at long wavelengths, has a very small resistive component and a reactive component corresponding to one-half the mass of air displaced by the sphere. (Note that in this report $-i\omega M$ instead of $+j\omega M$ corresponds to a mass reactance.) This is often called the "attached mass" of a vibrating body. For short wavelengths, or ka >> 1,

$$Z_a \simeq \frac{4\pi a^2 \rho c}{3} - i\omega M_s (1/ka)^2, \quad ka >> 1 \tag{B-11}$$

Thus, for high frequencies, the radiation impedance approaches a pure constant resistance equivalent to a $\rho c$ load on an area equal to one-third the surface area of the sphere. The "attached mass" reactive component decreases inversely as the square of frequency.

## OSCILLATING CYLINDER

In a manner similar to that employed above, Rschevkin derives the expression for the pressure $p(a, \phi)$ on the surface of a rigid cylinder of radius $a$ oscillating laterally with a velocity $V e^{-i\omega t}$. The results is (Reference 5)

$$p(a, \phi) = \frac{\rho c V e^{-i\omega t}}{C_1(ka)\, e^{i\gamma_1(ka)}} \left[J_1(ka) + i\, Y_1(ka)\right] \cos\theta \tag{B-12}$$

where $\theta$ is the circumferential angle, and the remaining terms are as defined in Equation 11 in the text.

The radiation reaction force per unit length of cylinder is given by

$$F_r = -a \int_0^{2\pi} p(a, \phi) \cos\theta \, d\theta \tag{B-13}$$

Substituting Equation B-12 into B-13, and dividing the force by the velocity of the cylinder, the radiation impedance per unit length of cylinder is found to be (Reference 5)

$$Z_a = \frac{\pi a \rho c \left[J_1(ka) + i\, Y_1(ka)\right]}{C_1^2(ka)\, e^{i\gamma_1(ka)}} = R_a - i\, X_a \tag{B-14}$$

where

$$\left.\begin{aligned} R_a &= \frac{\pi a \rho c}{C_1^2}\left[Y_1\left(J_2 - \frac{J_1}{ka}\right) - J_1\left(Y_2 - \frac{Y_1}{ka}\right)\right] \\ X_a &= \frac{\pi a \rho c}{C_1^2}\left[Y_1\left(Y_2 - \frac{Y_1}{ka}\right) + J_1\left(J_2 - \frac{J_1}{ka}\right)\right] \\ C_1^2 &= \left[\left(J_2 - \frac{J_1}{ka}\right)^2 + \left(Y_2 - \frac{Y_1}{ka}\right)^2\right] \end{aligned}\right\} \tag{B-15}$$

and the argument $ka$ is understood for the various Bessel Functions.

For long wavelengths, the radiation impedance is

$$Z_a \simeq 2\pi a \rho c \cdot \pi \frac{(ka)^3}{4} - i\omega M_c, \quad ka << 1 \tag{B-16}$$

where $M_c = \pi a^2 \rho$.

Thus, the radiation impedance is essentially equivalent to a mass reactance corresponding to the mass of air displaced by the cylinder.

For short wavelengths, the radiation impedance is very nearly a constant resistance equivalent to a $\rho c$ load on 1/2 the area of the cylinder, or

$$Z_a \simeq (2\pi a \rho c)/2 - i\omega M_c (1/ka)^2, \quad ka >> 1 \tag{B-17}$$

## PULSATING SPHERE AND CYLINDER

For comparison, the radiation impedance for the pulsating sphere and cylinder, as derived in References 1 and 5, are given below.

### Pulsating Sphere

The radiation impedance of a sphere of radius $a$, pulsating radially, is

$$Z_a = 4\pi a^2 \rho c \left[ \frac{(ka)^2 - i\,ka}{1 + (ka)^2} \right] \tag{B-18}$$

For long wavelengths, the radiation impedance is dominated by a mass ractance term equivalent to three times the mass displaced by the sphere, or

$$Z_a \simeq 4\pi a^2 \rho c (ka)^2 - i\omega \cdot 3\, M_s, \quad ka << 1 \tag{B-19}$$

and for short wavelengths, the impedance is essentially resistive

$$Z_a \simeq 4\pi a^2 \rho c - i\omega \cdot 3\, M_s (1/ka)^2, \quad ka >> 1 \tag{B-20}$$

## Pulsating Cylinder

The radiation impedance per unit length of a right circular cylinder of radius a pulsating radially is

$$Z_a = 2\pi a \rho c \left\{ \frac{[J_1 Y_0 - J_0 Y_1] - i [J_0 J_1 + Y_0 Y_1]}{J_1^2 + Y_1^2} \right\} \tag{B-21}$$

For long wavelengths,

$$Z_a \simeq 2\pi a \rho c \left(\frac{\pi ka}{2}\right) - i\omega M_c [\log_e (1/ka)^2], \quad ka << 1 \tag{B-22}$$

Note, that in this case, the effective mass increases without bound as the wavelength increases. However, the net mass reactance decreases since frequency decreases inversely as wavelength.

For short wavelengths, the load is resistive and equal to a $\rho c$ load on the total surface area.

$$Z_a \simeq 2\pi a \rho c, \quad ka >> 1 \tag{B-23}$$

The asymptotic expressions above are summarized in Table B-1. It is seen that the pulsating cylinder has the highest radiation resistance for long wavelengths, and either the pulsating sphere or cylinder has the highest resistance at short wavelengths. The pulsating sphere has the highest "attached mass" equal to three times the mass within its own volume for long wavelengths.

TABLE B-1

ASYMPTOTIC EXPRESSIONS FOR THE MECHANICAL RADIATION RESISTANCE AND REACTANCE OF PULSATING AND OSCILLATING SPHERES AND CYLINDERS

| Radiator | ka << 1 (Long Wavelengths) | ka >> 1 (Short Wavelengths) |
|---|---|---|
| **SPHERE** | | |
| Area = $S_s = 4\pi a^2$ | | |
| Mass = $M_s = \frac{4}{3}\pi a^3 \rho$ | | |
| Pulsating | $\begin{cases} R_a = S_s \rho c (ka)^2 \\ X_a \simeq \omega \cdot 3 M_s \end{cases}$ | $R_a \approx S_s \rho c$<br>$X_a = \omega \cdot 3 M_s (1/ka)^2$ |
| Oscillating | $\begin{cases} R_a \simeq S_s \rho c (ka)^4/12 \\ X_a \simeq \omega M_s/2 \end{cases}$ | $R_a \simeq S_s \rho c/3$<br>$X_a \simeq \omega M_s (1/ka)^2$ |
| **CYLINDER** | | |
| Area = $S_c = 2\pi a \cdot 1$ | | |
| Mass = $M_c = \pi a^2 \rho \cdot 1$ | | |
| Pulsating | $\begin{cases} R_a \simeq S_c \rho c (\pi ka/2) \\ X_a \simeq \omega M_c [\log_e (1/ka)^2] \end{cases}$ | $R_a \simeq S_c \rho c$<br>$X_a \rightarrow 0$ |
| Oscillating | $\begin{cases} R_a \simeq S_c \rho c \pi (ka)^3/4 \\ X_a \simeq \omega M_c \end{cases}$ | $R_a \simeq S_c \rho c/2$<br>$X_a \simeq \omega M_c (1/ka)^2$ |